

UNIVERSITY OF NAPLES FEDERICO II

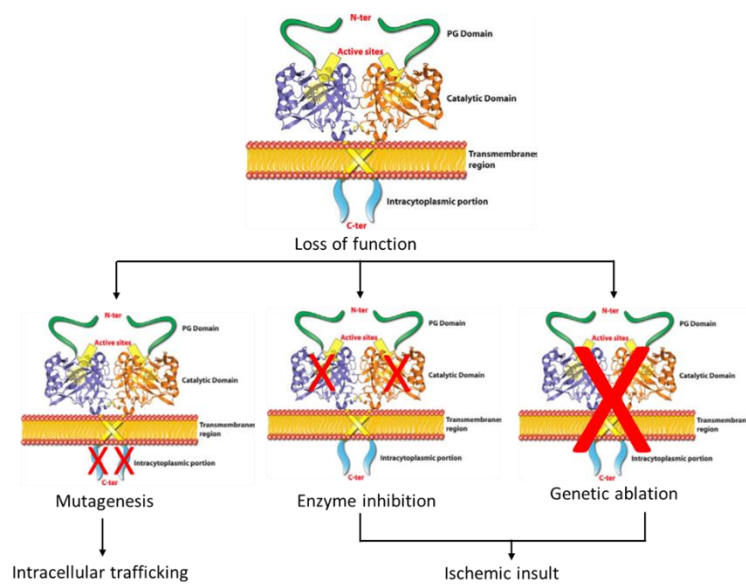
DOCTORATE IN MOLECULAR MEDICINE AND MEDICAL BIOTECHNOLOGY

XXXV CYCLE



Sara Amiranda

Loss-of-Function Analysis of Carbonic Anhydrase IX in Cellular and Animal Models



2019-2023

UNIVERSITY OF NAPLES FEDERICO II

**DOCTORATE IN
MOLECULAR MEDICINE AND MEDICAL
BIOTECHNOLOGY**

XXXV CYCLE



**Loss-of-Function Analysis of Carbonic Anhydrase IX
in Cellular and Animal Models**

Tutor
Prof./Dott. Nicola Zambrano

Candidate
Sara Amiranda

2019-2023

Index

Abstract	5
1. Introduction	6
1.1 Carbonic anhydrase family	6
1.2 CA IX gene and its products	8
1.3 CA IX functions in hypoxic cells.....	11
1.4 CA IX inhibitors	17
1.5 CA IX inhibition in diseases	19
1.6 Role in rRNA regulation and cell differentiation	21
1.7 Nucleocytoplasmic transport	22
1.8 Transmembrane protein maturation and sorting in eukaryotic cells	25
1.9 Molecular mechanisms of vesicular trafficking	27
2. Aims of the thesis	32
3. Results	33
3.1 CA IX proteins with mutated C-terminal sequences show impaired binding properties and altered subcellular distribution	33
3.2 Glycosidase shear-sensitivity analyses show incomplete maturation of the CA IX MUT1 protein and suggest its accumulation in the ER	40
3.3 CA IX MUT4 is enriched in Rab11-containing endosomes	43
3.4 Analysis of the distribution of CA IX proteins in hypoxic conditions	46
3.5 COPI-mediated retrograde trafficking from Golgi to ER is associated with the nuclear mis-translocation of CA IX WT....	48
3.6 CA IX subcellular localization in rat-derived primary neurons exposed to hypoxic and ischemic pre-conditioning	51

3.7 Genetic ablation of CA IX in mice reveals a detrimental role in neuronal cell survival	53
3.8 CA IX inhibition by C18 phenocopies the behaviour of Car9-deficient cortical neurons in the OGD/RX setting	55
3.9 CA IX expression is reduced in the neurons of ischemic rats ..	59
3.10 CA IX inhibition is neuroprotective in rat models of ischemia	64
4. Discussion.....	67
5. Conclusions	73
6. Materials and methods	75
7. Bibliography	84
8. Publications.....	96

Abstract

The human carbonic anhydrase IX (CA IX) is a hypoxia-induced transmembrane protein belonging to the α -CAs enzyme family. It has a crucial role in pH regulation in hypoxic cells and acts by buffering intracellular acidosis induced by hypoxia. Indeed, it is frequently expressed in cancer cells, where it contributes to tumour progression. CA IX is also localized in the nucleus, where it contributes to 47S rRNA precursor genes transcription, but the mechanism providing its nuclear translocation remains unclear.

Since CA IX is involved in a plethora of physio-pathological processes, we analysed CA IX functions in cellular and animal models more deeply, by implementing different loss-of-function strategies. Firstly, we analysed the results of specific mutations, targeting the C-terminal domain, on CA IX subcellular distribution, focusing on two loss-of-interaction mutants (MUT1 and MUT4) in the SH-SY5Y cell line; secondly, we characterized the impact of CA IX inactivation in ischemic processes, either with knock-out *ex vivo* murine primary neurons or with enzymatic inhibition in neurons and in rat brain.

The mutagenesis showed an altered subcellular localization of mutant forms, both unable to stably reside in the plasma membrane or in the nucleus, suggesting that CA IX nuclear translocation depends on its transit through secretory and endocytic pathways.

On the other hand, CA IX inactivation resulted to be protective in all the ischemic models studied. Although further characterization needs to be done to uncover the molecular mechanism underlying this protective role, this could pave the way for possible strategies for ischemic treatment, a condition with still too few therapeutic options.

1. INTRODUCTION

1.1 Carbonic anhydrase family

The carbonic anhydrases (CA), or carbonate dehydratases, belong to a superfamily of ubiquitous metalloenzymes found in both prokaryotes and eukaryotes, which are encoded by phylogenetically unrelated genetic families (Supuran 2008). There are six CA enzyme families known to date: α -CAs in Gram-negative bacteria, protozoa, algae, protozoa, green plants, and vertebrates; β -CAs found in algae, fungi, in both Gram-positive and Gram-negative bacteria, in chloroplasts of mono-cotyledons and di-cotyledons, and some Archaea; γ -CAs in Archaea and cyanobacteria; δ - and ζ -CAs appear to exist only in marine diatoms; η -CAs are present in protozoa (Supuran 2016b). To the so-called α -class belong all human CAs, which widely differ in subcellular localization, tissue distribution, and catalytic activity. Considering subcellular localization: in the cytosol reside CA I, II, III, VII, XIII; associated with the cell membrane there are CA IV, IX, XII, and XIV; in mitochondria reside CA VA, and VB, whereas CA VI is secreted into milk and saliva (Alterio et al. 2009). Looking at the catalytic activity: CAI, CAII, and CAIII isoforms have an intracellular catalytic site, whereas CA IV, CA IX, CA XII, and CA XIV catalyse the reaction extracellularly (Swietach et al. 2010). CA VIII, X, and XI are defined “CA-related proteins” owing to the lack of catalytic activity (Neri and Supuran 2011).

The substrate of these enzymes are some unusually simple molecules/ions chemically, because they catalyse the interconversion from carbon dioxide (CO₂) and water (H₂O) to bicarbonate (H₂CO₃) and protons (H⁺) and the reverse reaction:



HCO₃⁻ is poorly soluble in the lipid membranes and requires specific transporters, while CO₂ freely diffuses inside and outside the cell. For this,

the conversion of HCO_3^- to CO_2 results in its transportation across the cell membrane whereas the reverse reaction results in its blockade within the cell. The direction of this reaction depends on CO_2 levels and requires the participation of a Zn^{2+} ion, indispensable for the catalysis and present in the active site of nearly every CAs. Despite the absence of a catalyst this reaction can still occur, but it is too time-consuming to fulfill metabolic needs at physiological pH values, for CO_2 if generated in exceeding amounts may damage cellular components, whereas its conversion to HCO_3^- and H^+ , might tamper the cellular pH balance. Indeed, the typical catalytic efficiency is ranging from 10^4 and 10^6 reactions per second, while the reverse reaction is fairly slow, with a kinetic within the range of 15 seconds (Supuran 2016b).

CAs have a well-conserved catalytic domain prevalently composed of β -sheets, with a specific three-dimensional fold. Three histidine residues (His94, His96, and His119) are the main actors in the reaction since they coordinate with the Zn^{2+} ion, which is essential for catalysis and is localized in the deepest part of the active site. A hydrophilic region adjacent to the active site stabilizes it and binds CO_2 molecules. This molecule is nucleophilically attacked by a Zn-bound OH in the first stage of CA catalysis resulting in the formation of HCO_3^- . The HCO_3^- ion is eventually shuttled by an H_2O molecule and released in solution (Kciuk et al. 2022; Supuran 2008).

This reaction participates in central physiological and pathological processes connected with pH and CO_2 homeostasis/sensing such as respiration and transport of CO_2 and HCO_3^- , gluconeogenesis, lipogenesis, ureagenesis, electrolyte secretion, bone resorption, calcification, tumorigenicity, pathogen virulence and numerous other processes in various tissues and organs. Hence, many CAs are considered possible therapeutic targets to treat different disorders like obesity, cancer, epilepsy, and osteoporosis (Supuran 2008). Among all isoforms, CA IX and CA XII turned out to be remarkably interesting for their overexpression in many kinds of

cancer and association with radio- and chemotherapy (Pastorekova, Zatovicova, and Pastorek 2008).

1.2 CA IX gene and its products

The gene encoding for CA IX is located in region p12-p13 of chromosome 9, is 10.9 Kb long and consist of 11 exons and 10 introns (Nakagawa et al. 1998). The first exon encodes for the signal peptide and the proteoglycan-like domain (PG), exons 2-8 encode for the catalytic domain (CA), exon 10 for the transmembrane segment (TM), and exon 11 for the intracytoplasmic tail (IC) (Opavsky et al. 1996). Under appropriate conditions, CA IX gene is transcribed into a 1.5 Kb mRNA. Beside this mRNA, a truncated form named AS CA IX is generated by alternative splicing, with the loss of exons 8-9. This truncated form generates a 54 KDa protein with a diminished catalytic activity (since the loss of the C-terminal portion of CA domain) and is constitutively expressed at reduced levels (Barathova et al. 2008). The full-length variant is preponderant and generates a complete protein of 58 KDa, generally expressed in hypoxic tissues and tumours and in a limited number of normal tissues (Kaluz et al. 2009).

The promoter driving CA IX expression (from -173 to +31) contains six cis-acting regulatory elements: five Protected Regions (PRs) and one Hypoxia Response Element (HRE) between PR1 and the transcription start site. Except for PR4, all PR regions have a positive effect on transcription, more specifically PR1 and PR5 constitutively bind Sp1/Sp3 factors and PR2 binds AP-1 (Kaluz et al. 1999). The HRE sequence TACGTGCA contains HIF (Hypoxia Inducible-Factor) binding site, activated by HIF-1 factor. This activation is vital for recruiting the transcriptional machinery complex on CA IX promoter. For this reason, hypoxia, through the activation of HIF-1, is directly involved in the regulation of CA IX expression (Kaluz et al. 2009; Wykoff et al. 2000).

X-ray crystallographic studies have enabled us to describe CA IX as a transmembrane protein, with a sequence of 459 amino acids, divided into 4 domains. From N- terminus to C-terminus: the signal peptide (aa 1-37), a proteoglycan-like domain PG (aa 53-111) and the catalytic domain CA (aa 137-391) that constitute the extracellular portion; a transmembrane domain TM (aa 415-433) and a small intracytoplasmic tail IC (aa 434-459) that constitute the intracellular trait (Fig.1A) (Supuran et al. 2018; Supuran et al. 2010). Each domain is correlated to specific protein functions (Alterio et al. 2009). The PG domain, typical of CA IX, is the outermost and for this it is associated with cell adhesion and intracellular communications, reducing the binding E-cadherin/ B-catenin, thus promoting cell detachment. This domain also ensures a better enzymatic activity at acidic pH, for it contains negatively charged amino acids that can interact with the positively charged ones present in the active site, likely controlling substrate accession and/or participating in proton transfer reaction (Svastova et al. 2003). The CA domain is involved in cell growth and survival and, according to some evidence, it seems to be linked also with cell migration (Svastova et al. 2012). Finally, the IC domain appears to be essential for the correct enzymatic function for its localization. In fact, its mutations reduce cell adhesion, impair its interaction with other proteins involved in signal transduction, and withdraw extracellular environment acidification (Hulikova et al. 2009).

Further crystallographic studies on CA IX structure suggested that it could function as a symmetrical dimer (Fig.1B), which formation seems to be due to an intermolecular disulphide bridge at the level of Cys41 on both monomers presenting the N-terminus on the same side and the C-terminus on the opposite side. These studies further showed the occurrence of an intramolecular disulphide bond at the level of Cys119 and Cys229 and the presence of two glycosylation sites: N-glycosylation in the CA on Asn309 and O-glycosylation on the Thr78 of the PG domain. Moreover, its CA domain is described as a compact globular domain where the active site is

located in a large and conical cavity that extends from the surface to the core of the protein with the Zn^{2+} ion at its bottom side (Hilvo et al. 2008).

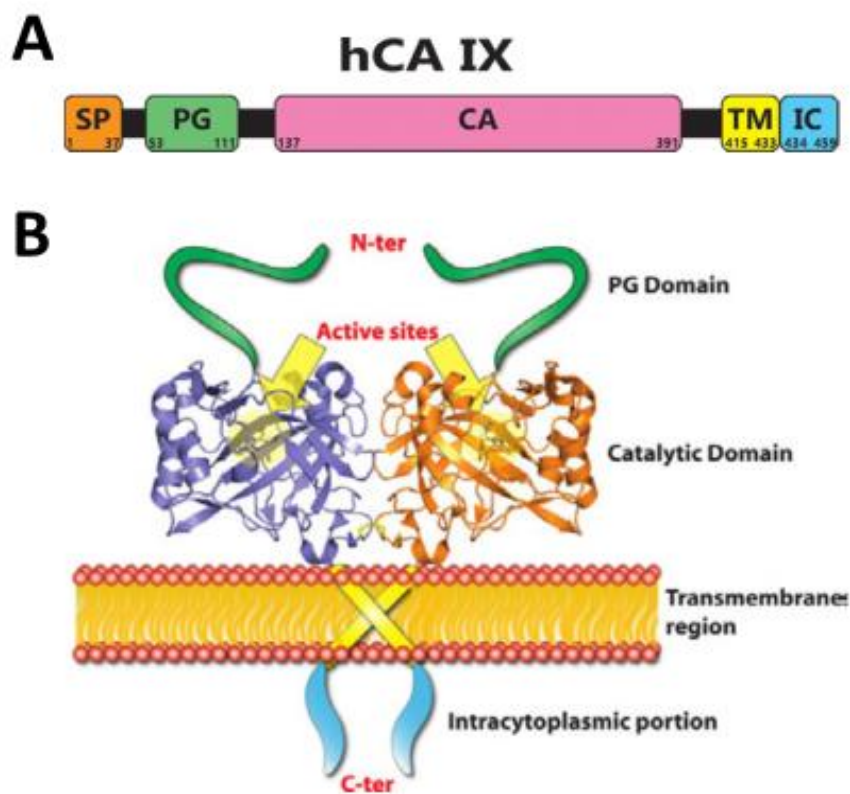


Figure 1: Schematic domain organization of hCA IX. **A)** the signal peptide (SP) in orange, the proteoglycan-like domain (PG) in green, the catalytic domain (CA) in pink, the transmembrane segment (TM) in yellow, and the intracytoplasmic tail (IC) in blue are represented. The numbers of the first and last amino acid of each domain are shown. **B)** Model showing the structural arrangement of the full-length CA IX dimer on the cell membrane, resulted by X-ray crystallographic studies. (Supuran 2018)

1.3 CA IX functions in hypoxic cells

Hypoxia is a condition of oxygen deficiency that can severely impair the brain and other tissue's normal functions since oxygen is necessary for aerobic metabolism. Solid tumours often contain regions of hypoxia and/or acidosis, caused primarily by aberrant tumour vasculature. The selective pressure created by this microenvironmental stress induces a spectrum of cellular responses leading to aggressive tumour phenotypes and correlates with cancer progression, malignancy, and treatment resistance (Pastorekova and Gillies 2019).

At the molecular level, these changes are principally determined by HIF-mediated reshaping of the transcriptional profile, which depends on the extent, duration, and severity of hypoxia and that includes, among other genes, CA IX (Svastova et al. 2004; Wykoff et al. 2000). In terms of structure, HIF-1 is a heterodimeric transcriptional factor composed of an oxygen-dependent α subunit and a constitutive β subunit. Among the three existent α subunits (1α , 2α , 3α) only HIF-1 α is capable to transactivate CA IX promoter (Huang and Bunn 2003). In normoxic conditions, HIF-1 α has a really short half-life and is rapidly addressed to proteasome-mediated degradation. This process is mediated by prolyl-hydroxylase (PHD) that hydroxylates the α subunit in Pro402 and Pro564 residues in presence of high O₂ levels. This enables the recognition and binding with von Hippel–Lindau protein (VHL), a member of the E3 ubiquitin ligase complex, which polyubiquitinates it, leading to its degradation via the proteasome. Conversely, in hypoxia, the PHD is inactive, for the lowering of O₂ levels, and unable to hydroxylate HIF-1 α that accumulates in the cell nucleus as a result. This allows the dimerization with HIF-1 β and the subsequent transactivation of targeted genes, containing the HRE in their promoter, such as VEGF, GLUT1/3, EPO1 and CA IX (Harris 2002) (Fig.2).

Nevertheless, there are some inconsistencies between HIF-1 α and CA IX expression. This discrepancy is explained by the different kinetic of the two proteins: the former is promptly degraded in normoxia and rapidly stabilized in hypoxia, whereas the latter is slowly activated and slowly degraded and takes several hours to be detectable. Accordingly, cells that have recently suffered hypoxic stress do not show appreciable levels of CA IX, while HIF-1 levels are undoubtedly high. On the other hand, cells that have experienced hypoxic stress followed by re-oxygenation present elevated levels of CA IX and low levels of HIF-1. Furthermore, CA IX expression can occur also in a HIF-independent manner. Indeed, the activation of the MAPK and PI3K pathways and upstream tyrosine kinases, namely SRC and RET also increase CA IX transcription (Pastorekova and Gillies 2019).

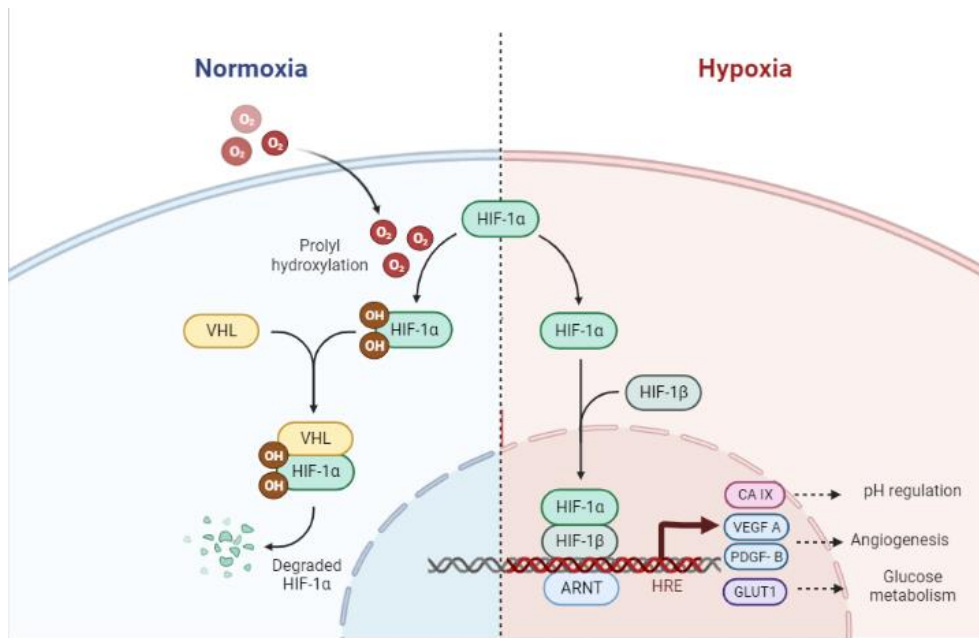


Figure 2: Hypoxia-induced HIF- mediated reshaping of the transcriptional profile. In normoxia HIF-1 α is rapidly hydroxylated by PDH, poly-ubiquitinated by VHL and degraded via proteasome. In hypoxia PDH is inactive allowing HIF-1 α accumulation in the nucleus, its dimerization with HIF-1 β and the transactivation of its target genes, like CA IX. These genes are involved in pH regulation, tumorigenesis, angiogenesis, and glucose metabolism. (Biorender)

Hypoxia triggers the metabolic shift toward anaerobic glycolysis that allows for sustained, though less efficient, energy generation in O₂ shortage (Gillies and Gatenby 2015). Notably, even in the presence of oxygen tumour cells rely on fermentative glycolysis, a phenomenon known as the Warburg Effect, or aerobic glycolysis (Vander Heiden, Cantley, and Thompson 2009). Glutaminolysis and glycolysis can further support the synthesis of biomolecules required to produce new cells during tumour expansion. To prevent the cytosolic accumulation of acidic metabolites like lactic acid, CO₂ and H⁺, and the subsequent prolonged intracellular acidosis, cells strengthen the activity of the pH balancing machinery and reroute the transmembrane ion fluxes (Parks, Chiche, and Pouyssegur 2011). This leads to extracellular acidosis that persists in tumour microenvironment because the acid metabolic waste is not effectively removed by the abnormal vasculature (Raghuhand, Gatenby, and Gillies 2003). The oncogenic metabolism, angiogenesis, invasion, autophagy, and metastasis are supported by acidosis (Rohani et al. 2019). Moreover, acidosis is a potent inhibitor of T cell effector functions and similarly to hypoxia, is linked with resistance to chemo-, radio- and immune therapies (Lardner 2001).

Diffusion of CO₂, export of H⁺ and lactate, production of HCO₃⁻ ions through the hydration of CO₂ and their subsequent importation usually lead to the removal of intracellular acidosis. In this scenario, CA IX assists pH regulation across the cell membrane through the acceleration of CO₂ hydration, thus promoting cell survival. In hypoxic cells this mechanism counteracts hypoxia-induced acidosis and contributes to the maintenance of physiological intracellular pH (pHi), acidifying the extracellular environment (pHe) (Parks, Chiche, and Pouyssegur 2011). To date, it is now well documented that it happens in spatial and functional coordination with lactate and proton-exporting monocarboxylate transporters (MCT), sodium-dependent bicarbonate transporters (NBC), and other pumps, ion exchangers, and transporters (Morgan et al. 2007; Jamali et al. 2015).

CA IX, with its extracellular domain, catalyses the conversion of CO_2 to H^+ and HCO_3^- (Fig.3). The adjacent NBC uploads HCO_3^- ions and transports them across the plasma membrane to the cytoplasm. Within the cell, HCO_3^- reacts with the H^+ resulting from various metabolic pathways. This reaction is mediated by intracellular CAs, especially CA II, and result in bicarbonate-mediated H^+ neutralization, with the formation of H_2O and CO_2 , which diffuses outside the cell. There it is converted into H^+ and HCO_3^- and another cycle starts (Pastorekova and Gillies 2019). This allows to obtain such pH values as to ensure metabolic processes, signalling, and proliferation. On the other hand, the H^+ generated by this reaction remain outside the cell and contributes to the acidification of the extracellular environment.

CA IX can further contribute to lactate export by a non-catalytic mechanism thanks to the cooperation of its PG domain with MCT complex, driving parallel proton flux and lactate extrusion out of the cell (Ames, Pastorekova, and Becker 2018). This causes further extracellular acidification, which supports extracellular matrix degradation and cancer cells invasiveness. The H^+ also guarantees drug resistance, considering that drugs are usually weak bases inactivated by protonation in an acid environment. This explains why tumours expressing CA IX are extremely aggressive (Supuran 2008).

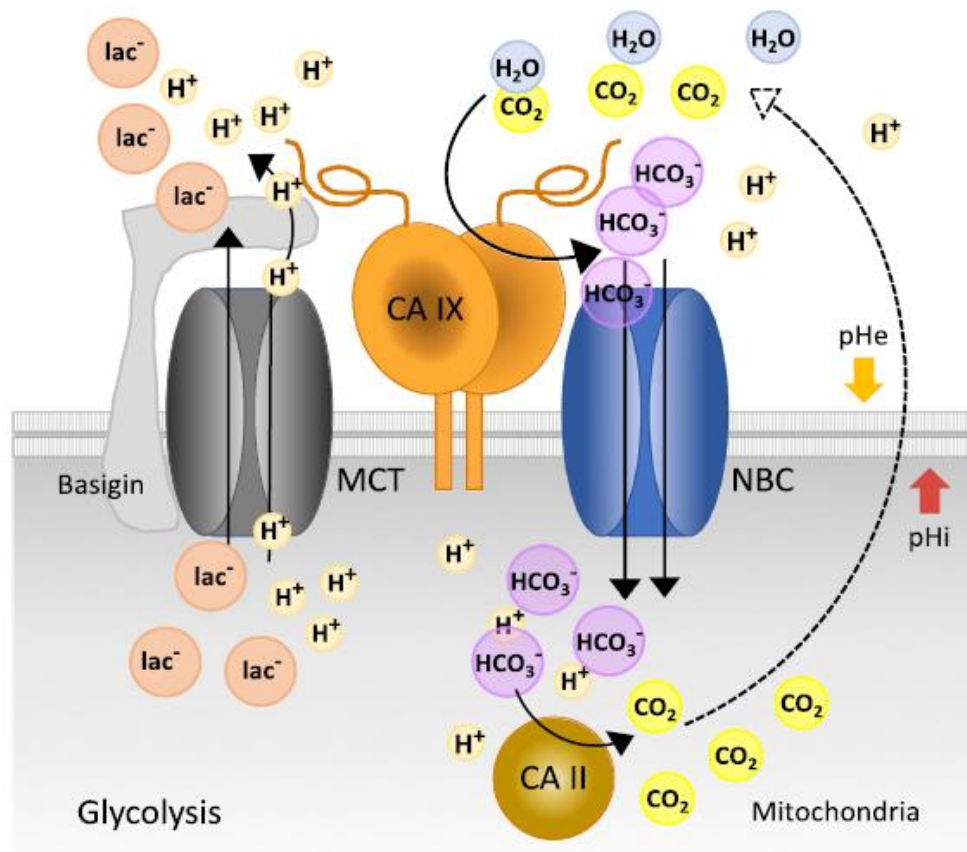


Figure 3: A schematic model of the role of CA IX in regulating pH in hypoxic cancer cells. This mechanism counteracts hypoxia-induced acidosis and contributes to the maintenance of physiological intracellular pH (pHi), acidifying the extracellular environment (pHe). To secure cell survival, by elimination of protons from the intracellular space, CA IX can interact with bicarbonate transporters and monocarboxylate transporters (Pastorekova and Gillies, 2019).

1.4 CA IX inhibitors

Understanding the structure and mechanism of action of CAs catalytic domain provided important perspectives in the design of CA IX selective inhibitors with potential diagnostic and therapeutic applications (Supuran et al. 2010). So far, two main strategies have been used to inhibit CAs, and in particular CA IX, based respectively on the discovery of small inhibitors and on the design of monoclonal antibodies and for both some molecules reached the clinical trial (Supuran 2016a).

Small molecule inhibitors can interact with the enzyme in diverse ways. The zinc binders include primary sulphonamides, some carboxylates and hydroxamates, dithiocarbamates, and related derivatives, and they directly coordinate to the zinc ion in the active site, thus replacing the nucleophile. Phenols, polyamines, some carboxylates, sulphocoumarins hydrolysed to sulfonic acid and thioxocoumarins are inhibitors that anchor to the non-protein zinc ligand and bind to the water molecule coordinated by the zinc ion. The inhibitors occluding the active site entrance are coumarins in hydrolysed form as 2-hydroxy-cinnamic acid derivatives and some of their derivatives and they act binding and occluding the entrance of the active site. Some carboxylic acid derivatives, on the other hand, bind outside the active site and block its entrance. Secondary/tertiary sulphonamides, some ethers, and several other compound classes inhibit CAs by a still unknown inhibition mechanism (Supuran et al. 2018).

The crucial problem of CA inhibition is the presence of a lot of isoforms with different localization and expression levels and the high similarity of their active site. The first class of CAIs, which comprises acetazolamide, methazolamide, dichlorphenamide, ethoxzolamide, and sulthiame, is as a matter of fact made up of highly efficient compounds acting in the nanomolar range, it has also well-characterized interaction in adduct with CA active site obtained through X-ray crystallographic structure, but

unfortunately, many of them inhibit indiscriminately most of the CA isoforms, hence their clinical use could lead to a range of undesired side effects (Alterio et al. 2009).

Much effort has been made to reduce the potential side effects and increase the selectivity for CA IX (De Simone, Alterio, and Supuran 2013). The first step was the design of membrane-impermeable compounds, which can inhibit specifically the membrane isoforms (CA IX and CA XII) without interacting with cytosolic and mitochondrial ones. Starting from these characteristics, many compounds with different modifications and/or substitutions have been analysed to increase functionality and selectivity (Supuran 2008). To this new class of carbonic anhydrase inhibitors (CAIs) belongs the sulphonamide compound 18, firstly described by Supuran (2008) and used in this study. Because of its positive charge and of the incorporation of pyridinium moieties, it discriminates between the membrane and the cytosolic CAs, because of its inability to cross the plasma membrane. A relatively recent generation of CAIs includes glycol-conjugated sulphonamides with membrane impermeability as well as specific inhibition of CAIX (Kciuk et al. 2022) or prodrugs, which are activated by acidification in the hypoxic environment (Anduran et al. 2020).

SLC-0111 is an ureido-benzene-sulphonamide inhibitor of CA IX and XII that can be used in the treatment of various tumours including, glioblastoma, breast, pancreatic and bladder cancer in cell culture (Mussi et al. 2022). SLC-0111 has recently finished a successful Phase I clinical trial for advanced and metastatic solid cancers characterized by hypoxic and acidic conditions. Currently, it is in Phase Ib/II clinical studies, both in monotherapy and in combination with other agents such as gemcitabine (McDonald et al. 2020). Moreover, it is under investigation in synergy with chemo-, radiation- and immuno- therapies, to reduce the adverse effect and overcome drug resistance, which leads to frequent relapses in cancer patients (Supuran 2021).

The selective inhibition of CA IX has been also achieved with the development of monoclonal antibodies (mAbs) targeting its active site, which showed to be effective in many ways, especially for anticancer therapies. The first mAb against CA IX is G250, known also by the tradenames Rencarex or Girentuximab. This antibody precisely recognizes CA IX catalytic domain and does not cross-react with other CAs isoforms, even the membrane-bound CA XII. The binding of G250 to its epitope causes antibody-mediated cell cytotoxicity of cancer cells, triggering immunity in the tumour niche. Moreover, it has long persistence within the cell for it is internalized by clathrin-coated vesicles and recycled by the perinuclear compartment (Zatovicova et al. 2010). This antibody showed a good safety profile, tolerability, and effectiveness in patients with metastatic renal cell carcinomas (RCC) in clinical Phase I and II (Bleumer et al. 2004; Siebels et al. 2011). Despite this initial success, a phase III trial to study the efficacy of Rencarex in RCC, did not show clinical benefit or improvement in patient survival, probably due to the age of the patients enrolled in the study. In addition to their role, mAbs can be combined with drugs to help their release in specific regions upon binding to their target or in combination with other anticancer therapy to improve their efficacy and overcome drug resistance in patients (Krasavin et al. 2020).

1.5 CA IX inhibition in diseases

As hypoxia is a key feature of tumours and has a pivotal role for cancer cell survival and metastasis, mainly because of the overexpression of CA IX, which ensures the acidification of the extracellular environment, ensuring intracellular pH stability, correlated to a worse prognosis (Ilardi et al. 2014). Due to its relatively low expression in normal tissues, CA IX inhibition represents a crucial strategy to selectively target hypoxic tumours, increasing apoptosis and reducing the invasiveness of cancer cells.

Beyond its well-known role in tumours, hypoxia is a key feature of other important pathological conditions. Among these, cerebral ischemia is a condition with still too few therapeutical options, therefore, since CA IX is involved in this condition, its inhibition could be used to manage ischemia (Bulli et al. 2021). Brain acidosis generates free radicals, and affects glutamate reuptake, glial cell activation and neuronal apoptosis, thus causing neuronal damage (Erra Diaz, Dantas, and Geffner 2018) leading to cerebral infarction such as oedema and blood-brain barrier dysfunction (Plum 1983). Skull stiffness limits the brain volume, so the presence of oedema is an aggravating factor in ischemic stroke because even the presence of small excess volumes leads to elevated intracranial pressure and compression of neural tissue and vasculature. Hence, the involvement of CA in the regulation of body fluid volumes creates a further opportunity to reduce ischemia-induced damage (Williamson et al. 2019). CA enzymatic activity inhibition has been related to enhanced production of the vasodilator molecule nitric oxide (NO) (Tuettenberg, Heimann, and Kempinski 2001). A first attempt was a study in rats that underwent permanent middle cerebral artery occlusion as a model of human ischemia and treated with both coumarins and sulphonamides derivatives. The neurological score was found improved, and the volume of infarction was found to be reduced in rats treated with specific CAI compared to the non-specific inhibitor acetazolamide even though a deeper investigation is needed (Di Cesare Mannelli et al. 2016).

The ubiquity and the variety of CAs isoforms reflect their involvement in many physiological processes, making CAIs potentially therapeutical not only for cancer but for a plethora of diseases. For the abundance of CAs in the kidney, the first CAI used was acetazolamide as a diuretic: it inhibits both cytosolic and membrane CAs, increasing the secretion of NaHCO_3 in the lumen, followed by an isotonic movement of water, with the result of increased diuresis (Trullas, Morales-Rull, and Formiga 2014). Similarly, since sodium bicarbonate is the main cause of high intraocular pressure

characteristic of glaucoma, CAIs, in particular acetazolamide, was used to effectively reduce this symptom. However, the long-term systemic administration of acetazolamide led to non-specific inhibition of CA isoforms, causing several side effects, so there were developed dorzolamide (Trusopt) and brinzolamide (Azopt), currently used for glaucoma treatment, which are sulphonamides soluble in water that can be administered topically as eye-drop, with reduced side effects (Sugrue 2000). The mitochondrial isoforms (CA V) provide HCO_3^- in several biosynthetic processes, so there is little evidence of CAIs use as anti-obesity drugs. Topiramate is an anti-epileptic drug that showed as side effects the loss of body weight and reduced fat gain in Zucker rats (Picard et al. 2000). Similarly, another anti-epileptic drug, zonisamide, showed potential use in therapy for some neuropathies, obesity, and eating disorders (Gadde et al. 2003). CAs are also abundant in the bone where they participate to inorganic matrix degradation, the use of inhibitors in rat osteoclasts showed increased bone resorption, which could pave the way to new anti-osteoporosis therapies (Riihonen et al. 2007). Moreover, in patients affected by juvenile arthritis, membrane-bound CAs were found in synovial fluid (Margheri et al. 2016), so it is currently under investigation the use of coumarins as anti-arthritic therapy (Bua et al. 2017).

1.6 Role in rRNA regulation and cell differentiation

Previous studies of our research group have characterized CA IX interactome, mostly composed by proteins containing the HEAT/ARM repeat domain and belonging to the nuclear transport machinery, such as exportin 1 (XPO1) and transportin 1 (TNPO1) (Buanne et al. 2013). Indeed, the discovery that CA IX could have an unusual nuclear function besides its conventional catalytic activity is relatively recent. Studies conducted by our group have also demonstrated a nuclear and nucleolar enrichment of this protein (Sasso et al. 2015). In detail, CA IX appears to be linked to rRNA 45S

promoters more in normoxic than hypoxic conditions. Moreover, CA IX and pre-rRNA 45S transcript are inversely related: in hypoxia the former increases whereas the latter is reduced. This could be attributable to CA IX interaction with XPO1, one of its major interactors. CA IX/ XPO1 complexes are scarce in normoxia and particularly enhanced in hypoxia. CA IX presence on rRNA promoter relates with pre-rRNA 45S transcript levels enhancement, typical of normoxic condition. Conversely, low levels of pre-rRNA 45S transcripts in hypoxia could be associated with CA IX- mediated decoy by its joining with XPO1, accountable for CA IX increasing in sub-nucleolar district.

Further analysis has suggested CA IX potential involvement in cellular differentiation processes too. Retinoic acid-induced cells differentiation in vitro showed not only a significative increase of CA IX protein levels but also nucleolar enrichment and reduction of rRNA levels when compared with non-differentiated cells. It is likely that the stimulation of cellular differentiation could drive rRNA regions heterochromatinization, thus inhibiting the access of CA IX to a potential DNA binding site. This would explain why, despite the presence of CA IX in the nucleolar district, its activity on the rRNA promoter remains ineffective (Sasso et al. 2015).

1.7 Nucleocytoplasmic transport

In eukaryotic cells the genetic material is enclosed inside the nucleus, separated from the cytoplasm by the nuclear envelope. Proteins working in the nucleus, involved in DNA replication and transcription, and mRNA, translated in the cytoplasm, demand a ceaseless import/export trafficking in and from the nucleus. This continuous interchange of material occurs through dedicated transport channels spanning the nuclear envelope, named the nuclear pore complex (NPC) (Hoelz, Debler, and Blobel 2011). This complex consists of 3 key structures: the cytoplasmic filaments, the nuclear basket and

a central core that connects the previous forming an aqueous channel. Every NPC is composed by about 30 different proteins, known as nucleoporins (Grossman, Medalia, and Zwerger 2012). Small water-soluble molecules up to 20 kDa diffuse easily through the NPC, whereas larger molecules need an active transport mediated by GTP-hydrolysis and transporters, the karyopherins- β . In humans, there are about 20 karyopherins- β , able to recognize various cargo signal sequences thanks to conformational changes. These proteins contain the HEAT repeat domain and can be divided into importins and exportins, respectively mediating import and export from the nucleus (Conti, Muller, and Stewart 2006).

Molecules needing to be transported into the nucleus contain a nuclear localization signal (NLS), classically represented by three or five positively charged amino acid residues, recognised by importins. This sequence can be monopartite as in the case of SV40 large T antigen (PKKKRKV), or bipartite such as that of nucleoplasmin (AVKRPAATKKAGQAKKKKLD). The former contains a single cluster of positively charged residues, whereas the latter has two clusters of positively charged amino acids, spaced by 10-12 residues (McLane and Corbett 2009). In the cytoplasm, importins recognize and bind the cargo molecules by either direct or indirect interaction, through an adaptor, and translocate them into the nucleus. Importin- β , known as karyopherin- β 1, contains 19-20 HEAT-repeats and imports molecules presenting the canonical NLS, not directly, but through an adaptor, the importin- α . This protein, known also as karyopherin- α , directly binds the cargo protein with an NLS-binding domain formed by 10 ARM repeats. It binds the importin- β and the cargo respectively through the importin- β binding domain and the NLS-binding domain (Bednenko, Cingolani, and Gerace 2003; McLane and Corbett 2009).

On the other hand, exportin cargo molecules that need to be carried out of the nucleus contain a nuclear export signal (NES), rich in hydrophobic

amino acids, such as leucine. In the nucleus, cargoes are bound by exportins, pass through the NPC, and are finally released in the cytoplasm. The NES-binding domain of exportins, e.g. exportin-1, is made of 20 HEAT repeats, organized in a ring structure, allowing its interaction with the cargo and the NPC, likewise the importins (Kutay and Guttinger 2005). Among known exportins, not all are bound to protein export. Indeed, exportin-t and exportin-5 are implicated in RNA transport toward the cytosol, respectively for tRNA and pre-miRNA (Leisegang et al. 2012). Human XPO1 can be inhibited by Leptomycin B (LMB), an unsaturated fatty acid that blocks its NES binding site by covalent modification of cysteine. In this way, molecules involved in nucleocytoplasmic trafficking are trapped in the nucleus (Rahmani and Dean 2017).

The nucleocytoplasmic shuttling is finely regulated by the Ran (Ras-related nuclear protein) GTPase nucleotide cycle. Ran is a small monomeric protein belonging to the Ras superfamily that has an intrinsic GTPase activity, i.e., the spontaneous hydrolysis of GTP to GDP. The interconversion between the GTP-bound status and the GDP-bound is referred to as Ran cycle and depends on Ran-specific proteins. The Ran guanine nucleotide exchange factor (RanGEF or RCC1) converts RanGDP into RanGTP. The intrinsic GTPase activity of Ran is triggered by a Ran GTPase activating protein (RanGAP), with the help of Ran-binding protein (RanBP) which facilitates the formation of the complex. The Ran cycle closes when the GTPase-activation converts the RanGTP to RanGDP. There is a different distribution of Ran between the two compartments: RanGTP is enriched in the nucleus, whereas RanGDP is concentrated in the cytoplasm. This compartmentalization depends on the activity of proteins controlling the nucleotide state of Ran: RanGAP is present in the cytoplasm, while RanGEF is in the nucleus associated with the chromatin (Weis 2003).

In the nuclear import, importins bind the cytosolic cargo molecules and translocate to the nucleus. There the complex dissociates consequent upon Importin1/RanGTP binding and the cargo is released. This newly formed complex returns to the cytoplasm, where RanGAP promotes the hydrolysis of GTP in GDP, Ran is released, and importins are free to start another cycle. Nuclear export occurs in an analogous way. The binding of RanGTP stabilizes the complex XPO1/cargo that passes through the NPC and leaves the nucleus. In the cytosol, the RanGAP-promoted exchange from GTP to GDP causes the dissociation of this complex. RanGDP is then associated with NTF2 and is recycled back to the nucleus where is converted by RCC1 in RanGTP and a further export cycle begins (Weis 2002).

1.8 Transmembrane protein maturation and sorting in eukaryotic cells

Protein synthesis is guided by information carried by mRNA molecules and is performed either at the level of free ribosomes (cytoplasm) or at the level of membrane-bound ribosomes (rough endoplasmic reticulum, RER). The latter are engaged in the synthesis of proteins that are being concurrently translocated into the endoplasmic reticulum (ER), whereas the former synthesize all other proteins. Proper protein folding depends on their amino acidic sequence and is essential for the right function (Alberts 2015).

The eukaryotic cell is divided into functionally distinct, membrane-enclosed compartments, each with its own characteristic set of proteins and molecules. These compartments are in dynamic communication through vesicle secretory pathways, a complex distribution system that transports specific products in the different compartments. Every newly synthesized protein must reach the correct subcellular district where it can exert its specific function. This is possible for the presence of sorting signals in their sequence, which are recognized for complementarity by sorting receptors on vesicles, which deliver that specific protein to the right organelle. For their

part, vesicles contain molecular information that directs them to the right target compartment, and their movement is due to the exploitation of specific intracellular filaments, like the microtubules, as railways. Proteins that function in the cytoplasm remain there after their synthesis due to the absence of signal sequence (Mellman and Warren 2000).

According to the proposed transport model for transmembrane glycoproteins, such as CA IX, the first step in the biosynthetic pathway is represented by their synthesis in the RER and the subsequent transport to the Golgi apparatus. In the ER lumen takes place protein folding and oligomerization, formation of disulphide bonds, and addition of N-linked oligosaccharides on Asn residues. The pattern of N-linked glycosylation denotes the degree of protein folding, in this way only properly folded proteins can leave the ER (Aebi 2013). Correctly folded and assembled proteins in the ER are directed through the cis-Golgi apparatus, where protein maturation continues. Indeed, the cis- and medial- Golgi apparatus are the sites where O-linked glycosylation on Ser/Thr residues occurs and where glycosaminoglycan chains are added to core proteins (Stanley 2011). The finished proteins arrive in the trans-Golgi network, where they are packed in transport vesicles and dispatched to their specific destinations in the cell. After vesicle fusion with the plasma membrane, the glycoproteins become integral proteins of the cell membrane, with sugar residues exposed only on the extracellular side (Ikonen and Simons 1998).

It is now well known in literature that the vesicular trafficking is defined *anterograde transport*, where vesicles proceed in the ER-Golgi, cis-trans direction, is counteracted by a *retrograde transport*, or retrieval pathway, where vesicles flow in the opposite direction, trans-cis or even Golgi-ER. This pathway allows firstly to bring the mistakenly transported proteins back to the appropriate compartment and secondly to restore the correct localization of the Golgi glycosylases (Lee et al. 2004).

The transport that leads inward from the cell surface starts with the process of endocytosis, in which cells ingest fluid, molecules, and particles. In this process, localized regions of the cell membrane invaginate and pinch off to form endocytic vesicles. Once generated, most endocytic vesicles blend in with the early endosome, a common receiving compartment functioning as the primary sorting station for cargoes. From the tubular portions of the early endosome originate vesicles that recycle endocytosed cargo back to the cell membrane directly, or via recycling endosomes indirectly. Recycling endosomes can store proteins for as long as necessary until they are needed. In a process called *endosome maturation*, late endosomes originate from a specific segment of the early endosomes. This process changes the composition of the proteins of the endosome membrane, which in some sections invaginates and integrates within the organelles as intraluminal vesicles, which contains membrane protein designed for degradation, meanwhile the endosome itself travels along microtubules toward the inner part of the cell, near to the nucleus. As an endosome matures, it ceases the recycling to the membrane and irrevocably commits the residual contents to deterioration. The fusion of late endosomes among themselves and with lysosomes generates the endo-lysosomes, which degrade their content (Doherty and McMahon 2009).

1.9 Molecular mechanisms of vesicular trafficking

Vesicle transport mediates a continuous exchange of components between chemically distinct, membrane-enclosed compartments that collectively comprise the secretory and endocytic pathways. Most transport vesicles originate from specialized membrane regions, where they emerge as coated vesicles, with proteins covering their cytosolic surface. The coat has two main functions, reflected in a common two-layered structure. First, an inner coat layer selects specific membrane proteins and concentrates them in

a specialized area, which will eventually give rise to the vesicle. Second, an outer coat layer assembles into a bent, basketlike reticulate that distorts the membrane patch, thereby shaping the vesicle. Before the vesicles fuse with a target membrane, they lose their coat, as is required for the interaction and fusion of the two membranes (Faini et al. 2013).

There are three well-characterized categories of coated vesicles, clathrin-coated, COPI-coated, and COPII-coated, used for a different kinds of transport (Gomez-Navarro and Miller 2016). For example, the transport from the plasma membrane and Golgi apparatus are mediated by clathrin-coated vesicles, whereas the transport between the ER and the Golgi apparatus is normally mediated by COPI- and COPII-coated vesicles. More specifically, COPI-coated vesicles bud from Golgi cisterns and COPII-coated vesicles from the ER. To balance the trafficking to and from a compartment, the assembly of the coat proteins must occur only when and where needed. Local synthesis of specific phosphoinositides creates binding sites that trigger coat assembly and vesicle formation (De Craene et al. 2017). Furthermore, almost all steps in vesicle transport depend on numerous GTP-binding proteins that control vesicle budding, docking, and fusion in both the spatial and temporal aspects. For instance, the coat-recruitment GTPases, including Sar1 (Secretion Associated Ras Related GTPase) and the ARF (ADP Ribosylation Factor 1) proteins, regulate coat assembly (GTP-bound) and disassembly (GDP-bound) (Donaldson and Jackson 2011).

To ensure an orderly vesicles flow, they must highly accurately recognize the appropriate target membrane for fusion. The distinctiveness of targeting is provided by surface markers displayed by all transport vesicles, which identify them by their origin and type of cargo. In return, the target membranes exhibit complementary receptors which recognize the right markers. This key process occurs in two steps. Firstly, Rab proteins and Rab effectors direct the vesicle to specific spots on the proper target membrane

(Stenmark 2009). Secondly, SNARE (Soluble NSF Attachment protein Receptor) proteins and SNARE regulators mediate the fusion of the lipidic bilayers (Jena 2011).

To each organelle of the endocytic or secretory pathway is associated one or more Rab proteins (Fig.4). The highly selective distribution across these membrane systems is what makes Rab proteins perfect molecular markers for identifying each type of membrane and guiding the flow of vesicles between them. The assembly and disassembly of Rab proteins and their effectors in specialized membrane domains is dynamically controlled by GTP binding and hydrolysis. In the GDP-bound state, they are inactive and bound to a Rab-GDP dissociation inhibitor that keeps them soluble in the cytosol. Conversely, in the GTP-bound state, they become active and strongly associated with an organelle membrane or a transport vesicle through the exposure of a lipid anchor. Membrane-bound Rab-GEFs turn on Rab proteins on both transport vesicles and target membranes. Once activated, Rabs can bind to other proteins, the Rab effectors, which are the downstream mediators of vesicle trafficking, membrane tethering and fusion (Pfeffer 2017).

The endosomal membrane is a striking example of how different Rab proteins and their effectors create multiple specialized membrane domains, each fulfilling a particular function. Thus, meanwhile the Rab5 membrane domain receives incoming endocytic vesicles from the cell membrane, distinct Rab11 and Rab4 domains in the same membrane organize the budding of recycling vesicles, returning proteins to the plasma membrane, respectively slow and fast recycling (Stenmark 2009). A Rab domain can be replaced by a different Rab domain, thereby changing the identity of an organelle. For example, over time, Rab5 domains on endosomal membranes are displaced by Rab7 domains. This converts the early endosome, marked by Rab5, into a late endosome, marked by Rab7. Because Rab effectors

recruited by Rab7 are different from those recruited by Rab5, this reprograms the compartment (Pfeffer 2013).

Once a transport vesicle has been tethered to its target membrane, it unloads its cargo by membrane fusion. This process is highly energetically unfavourable and requires specialized proteins that overcome this energy barrier and catalyse this fusion: the SNARE proteins. Complementary v-SNARE proteins on transport vesicles and t-SNARE proteins on the target membrane form stable trans-SNARE complexes, which force the two membranes into close apposition so that their lipid bilayers can fuse. Since v- and t-SNARE pairing is highly specific, the SNAREs provide an additional layer of specificity in the transport process, ensuring that vesicles fuse only with the correct target membrane (Jena 2011).

2. Aims of the thesis

CA IX, as a marker of cellular responses to hypoxia and of therapeutic resistance exerted by hypoxic tumours, is deeply characterized in cancer. There is still limited knowledge on its functions following acute ischemic insults and tissue reoxygenation, which characterize stroke and additional organ infarctions. The experimental background on CA IX available in the hosting laboratory and the established network of scientific collaborations convinced me to undertake an experimental plan, based on loss-of-function strategies, to hit CA IX via targeted mutagenic design, gene ablation, and enzyme inhibition, with the aim to contribute to the preliminary characterization of CA IX potential involvement in the responses to ischemic/reoxygenation damages *in vitro* and *in vivo*.

The mutagenic design was exploited by specifically targeting the C-terminal region of CA IX, the one which is involved in the interactions with intracellular proteins, among which the several components of the nucleocytoplasmic machinery; the main intent for that design, was to clarify the complex subcellular trafficking of CA IX in mammalian cells. The gene ablation strategy accounted on the isolation and characterization of *ex vivo* cellular models of primary neurons and stabilized embryonic fibroblasts from a murine *Car9*-knockout model. Finally, the enzyme inhibition relied on the availability of a membrane-impermeant inhibitor of carbonic anhydrases, able to act on extracellular CAs, such as CA IX and CA XII.

The complementary information emanating from the experimental efforts represented the intent to provide a basis to consolidate, on one hand, the knowledge on CA IX functions in the ischemia/reperfusion damages and, on the other hand, the therapeutic potential of its modulation in stroke.

3. Results

3.1 CA IX proteins with mutated C-terminal sequences show impaired binding properties and altered subcellular distribution

Previous studies conducted in our laboratory had characterized CA IX interactome, which is mostly composed of proteins containing the HEAT/ARM repeat domain; most of the CA IX protein ligands were found to belong to the nuclear transport machinery (Buanne et al. 2013). It was also shown that among CA IX binding partners, also the Cullin-associated NEDD8-dissociated protein 1 (CAND1) protein was represented, a factor participating to both gene transcription and assembly of SCF (Skp, Cullin, F-box) ubiquitin ligase complexes (Duda et al. 2011) CAND1 was also reported as contributing to CA IX stabilization (Buanne et al. 2013). Competition analysis previously showed that the C-terminal sequence of CA IX is necessary and sufficient for binding to the members of its interactome, CAND1, TNPO1, and XPO1 (Buanne et al. 2013). Advanced approaches like surface plasmon resonance and molecular modelling were used to uncover the details of the interaction between CA IX and CAND1, as a representative example (Buonanno et al. 2017). These studies confirmed previous findings regarding the minimal portion of CA IX protein required for the binding with its interactors, corresponding to the C-terminal sequence Leu418 –Ala459 of CA IX (Buanne et al. 2013), and contributed to generate structural details on the CA IX residues involved in this interaction. Modelling analysis and binding measurements of CA IX identified the peptide string from Leu418 to Ala459 as critically involved in the interactions with CAND1 (Buonanno et al. 2017).

The structural model of CA IX interaction with CAND1 and with the additional ligands was validated by means of site-directed mutagenesis followed by co-precipitation experiments, in which the ectopically expressed wild-type and mutant CA IX proteins were assayed for binding to selected

interactors. Mutations in the CA IX full-length protein were designed, with the purpose to disrupt either the van der Waals or the electrostatic interactions responsible for the binding to CAND1 (Buonanno et al. 2017). In more detail, the Leu423 and Thr427 residues involved in van der Waals interactions were mutagenized to arginine (Leu423/Arg-Thr427/Arg) to generate CA IX MUT1. Additionally, residues Arg436, Arg440, and Arg441, localized in the C-terminal tail and involved in strong electrostatic interactions, were mutagenized into alanine or glutamic acid (Arg436/Glu-Arg440/Glu; Arg436/Ala-Arg440/Ala; Arg436/Glu-Arg441/Glu; Arg436/Ala-Arg441/Ala) to generate respectively CA IX MUT2, CA IX MUT3, CA IX MUT4 and CA IX MUT5 (Table 1).

HEK-293 cells were transfected with plasmids driving the expression of wild-type CA IX and its mutants with C-terminal, in-frame Strep-Tag, to facilitate their enrichment on the beads, following ectopic expression in cultured cells. The co-precipitation analysis visualized by western blot showed that all the mutations resulted in the loss of interaction with CAND1, XPO1 and TNPO1 (Fig.5), whereas the wild-type CA IX protein was keeping its expected binding ability. These results highlighted that the designed mutant sites were crucial for CA IX interaction with its endogenous ligands.

Table 1: CA IX mutants and the corresponding site-specific mutations

Name	Mutated sites
CA IX MUT1	Leu423/Arg-Thr427/Arg
CA IX MUT2	Arg436/Glu-Arg440/Glu
CA IX MUT3	Arg436/Ala-Arg440/Ala
CA IX MUT4	Arg436/Glu-Arg441/Glu
CA IX MUT5	Arg436/Ala-Arg441/Ala

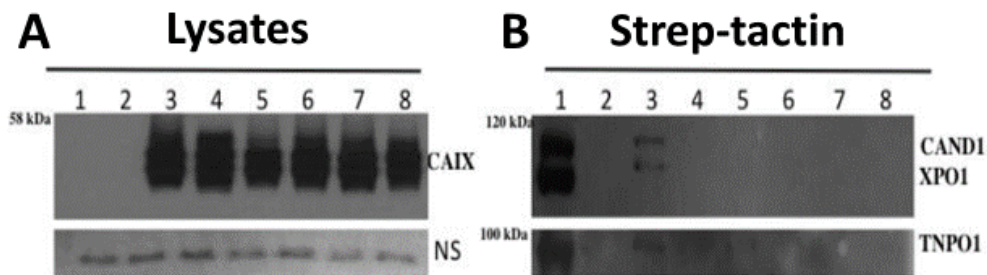


Figure 5: Co-precipitation experiments for binding properties evaluation of wild-type and mutant CA IX proteins with endogenous ligands. A) Western blot of HEK-293 lysates: 1) cells 2) mock transfected; 3) CA IX WT transfected; 4) CA IX MUT1 transfected; 5) CA IX MUT2 transfected; 6) CA IX MUT3 transfected; 7) CA IX MUT4 transfected; 8) CA IX MUT5 transfected. **B)** Pull-down analysis of CA IX WT and its mutant forms with CAND1, XPO1, TNPO1 through western blot.

Besides the biochemical evidence for defective binding properties of the mutant proteins, we hypothesized that lack of interaction with the natural CA IX ligands could generate defects in cellular trafficking. Thus, the representative mutant CA IX proteins CA IX-MUT1 (Leu423/Arg-Thr427/Arg) and CA IX-MUT4 (Arg436/Glu-Arg441/Glu), hitting the relevant peptide strings involved in the binding, were selected for subcellular localization analysis in the human neuroblastoma SHSY-5Y cell line.

The immunofluorescence analysis of the CA IX proteins exogenously expressed in SHSY-5Y cells (Figure 6A) confirmed a strong membrane signal for the wild-type protein, in contrast with the two mutant proteins, where this prominent localization was lost in favour of intracellular accumulations. Namely, the CA IX MUT1 protein showed a very intense intracellular signal, involving subcellular structures resembling the ER. CA IX MUT4 protein generated intracellular accumulations too, according to a distribution that would seem to highlight vesicles, located mostly in the perinuclear area and below the cytoplasmic membrane. As expected, the CA IX wild-type protein showed a weak nuclear presence, which was partially lost, in the case of CA IX MUT 1, and undetectable for the CA IX MUT4 protein; both mutant proteins showed, however, a perinuclear accumulation. In light of these results, the mutant proteins clearly showed altered subcellular distributions, compared to the wild-type CA IX protein. Even more interestingly, the subcellular distribution of the two mutant proteins differed deeply from each other.

Membrane proteins, including CA IX, frequently show nuclear localization in cell cultures (Buanne et al. 2013; Sasso et al. 2015); in order to evaluate the potential trafficking of the mutant proteins through the nuclear compartment, we performed immunofluorescence experiments in SHSY-5Y cells after having treated the cell cultures with LMB, an inhibitor of nuclear export. Thus, the nuclear accumulation of proteins resulting from LMB

treatment would provide an indication of their transit through the nuclear compartment. In the Panel B of Figure 6, a control experiment is shown, in which the EGFP protein fused to a canonical NES was normally excluded from the nucleus, while it accumulated in the nuclear compartment after treatment with LMB. As expected, wild-type CA IX showed straightforward evidence of nuclear accumulation; however, both MUT1 and MUT4 CA IX proteins showed limited evidence for nuclear representation upon treatment with LMB, indicating their impairments also in their nuclear trafficking.

To further investigate the different cellular localizations of the mutant proteins, we performed co-localization studies with well-known markers of intracellular structures, i.e., calreticulin for ER (Figure 7A) and golgin for Golgi apparatus (Figure 7B). In the case of wild-type CA IX, the lack of colocalization with the ER marker and the limited dimensions of the CA IX-comprising Golgi apparatus suggested the occurrence of a rapid trafficking through these structures while reaching the plasma membrane. The CA IX MUT4 protein showed significant co-localization, neither with calreticulin, nor with golgin. A more pronounced match of the CA IX MUT1 protein was, instead, clear with calreticulin with no match observed with the golgin marker, supporting the possibility that CA IX MUT1 accumulated into the ER. In agreement with the latter evidence, cells transfected with the CA IX MUT1 protein showed increased accumulation of GRP78 (BiP), a marker of ER stress (Figure 7C).

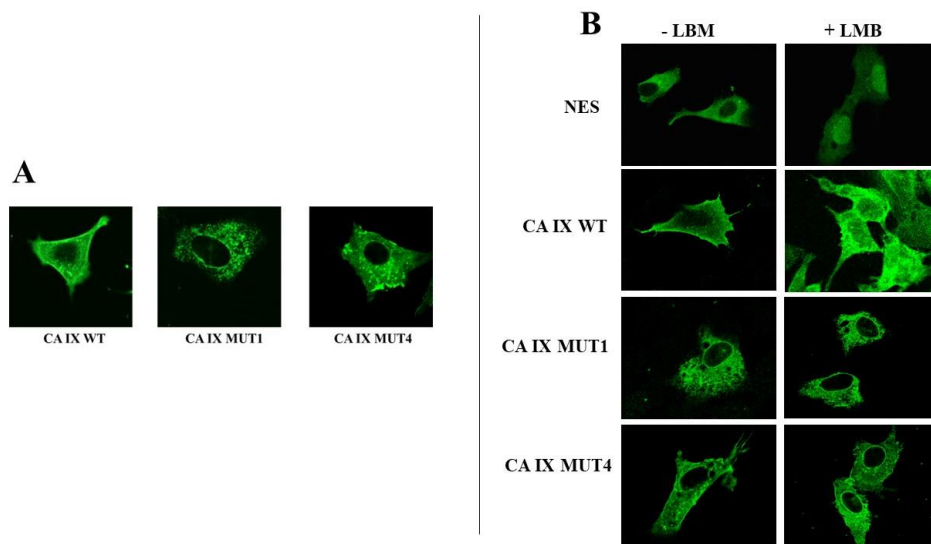


Figure 6. Localization studies of CA IX WT and its mutant forms in the human neuroblastoma SHSY-5Y cell line. **A)** Immunofluorescence analysis of CA IX WT, CA IX MUT1, and CA IX MUT4 in SHSY-5Y cells using monoclonal CA IX specific antibody VII:20 (green). Both mutants show a different intracellular localization compared to the WT protein. **B)** Immunofluorescence assay of CA IX WT, CA IX MUT1, or CA IX MUT4 was performed using transfected SHSY-5Y cells with or without leptomycin B (LMB) treatment for 5 hours at a final concentration of 20 ng/mL, or with 70% methanol as negative control. As positive control, a plasmid driving expression of GFP protein with nuclear export signal (NES) sequence was used. Cells transfected with CA IX WT and exposed to LMB showed enriched nuclear representation. Cells transfected with CA IX MUT4 showed a weak nuclear enrichment, whereas in MUT1 the treatment resulted in undetectable nuclear accumulation.

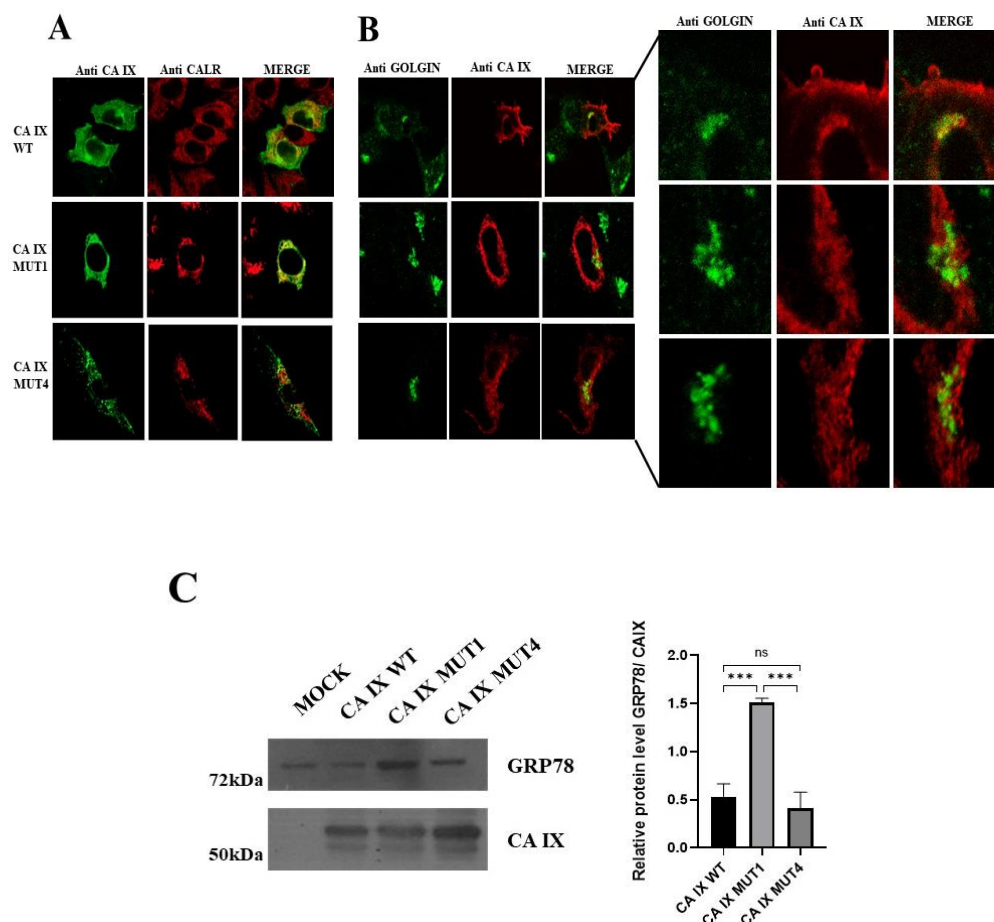


Figure 7. Co-localization studies of CA IX and its mutants with endoplasmic reticulum and Golgi apparatus markers in SHSY-5Y cells. **A)** CA IX (green) and calreticulin (red) were visualized by confocal fluorescence microscopy using specific antibodies. The merged images show straightforward evidence of CA IX co-localization with calreticulin by CA IX MUT1 protein. **B)** In this panel, CA IX is shown in green and golgin in red. The two mutants do not show significant co-localization with golgin, while a modest presence is detected for the WT protein. **C)** Unfolded protein response in the endoplasmic reticulum is shown by GRP78 expression levels in lysates of SH-SY5Y cells mock-transfected, or transfected with CA IX WT, MUT1, and MUT4 expression vectors. The Western blot analysis shows a significant increase of GRP78 levels in SH-SY5Y cells overexpressing CA IX MUT1. CA IX protein in the same lysates is used as normalizer. Statistics were performed by unpaired t-test (** $p < 0.005$)

3.2 Glycosidase shear-sensitivity analyses show incomplete maturation of the CA IX MUT1 protein and suggest its accumulation in the ER

The observed findings involving CA XI MUT1 could be associated to an altered maturation of the mutant protein; thus, to verify the actual transit of the wild-type and mutant CA IX proteins through the ER and the Golgi apparatus, we performed sensitivity experiments to glycosidase shear. It is in fact well known that CA IX is a substrate for N-glycosylation, which occurs in the ER, at the residue Asn309, and for O-glycosylation on Thr78 (Hilvo et al. 2008).

The analysis of N-glycosylation of the three proteins was performed by enzymatic digestion with the enzyme Endoglycosidase H (Endo H). This enzyme cuts between two N-acetylglucosamine residues of a sugar chain bound to asparagine, generating a truncated sugar molecule, consisting of a single N-acetylglucosamine residue bound to Asn. Endo H selectively digests chains with a high content of mannose and simple hybrids (typical of glycoproteins in transit in the ER) but is not able to cut complex oligosaccharides. N-glycosylation analysis was performed on the immunoprecipitation-enriched proteins CA IX WT, CA IX MUT1, and CA IX MUT4. The results in Figure 8A show that all the proteins undergo an N-glycosylation, since they all showed a shift in the electrophoretic migration, in comparison to the corresponding undigested controls.

Following enzymatic digestion with O-glycosidase, no differences in migration were observed between the treated or untreated samples (Figure 8B, upper panel). The lack of digestion of CA IX WT with O-glycosidase led us to think that the enzyme could not work due to sialic acid residues protecting the potential cleavage sites. For this reason, we made use of neuraminidase, which removes the sialic acid residues. In the bottom panel of figure 8B, it is observed a slight shift in electrophoretic migration, when compared with undigested samples, for both CAIX WT and CA IX MUT4 proteins, suggesting that they were O-glycosylated; no shift was detected,

however, in the case of the CA IX MUT1 protein. Taken together, these results show that all the CA IX proteins evaluated actually transit through the ER and that only the CAIX WT and CA IX MUT4 are capable to pass through the ER and undergo post-translational modifications in the Golgi apparatus; accordingly, we concluded that the CA IX MUT1 protein accumulates within the ER.

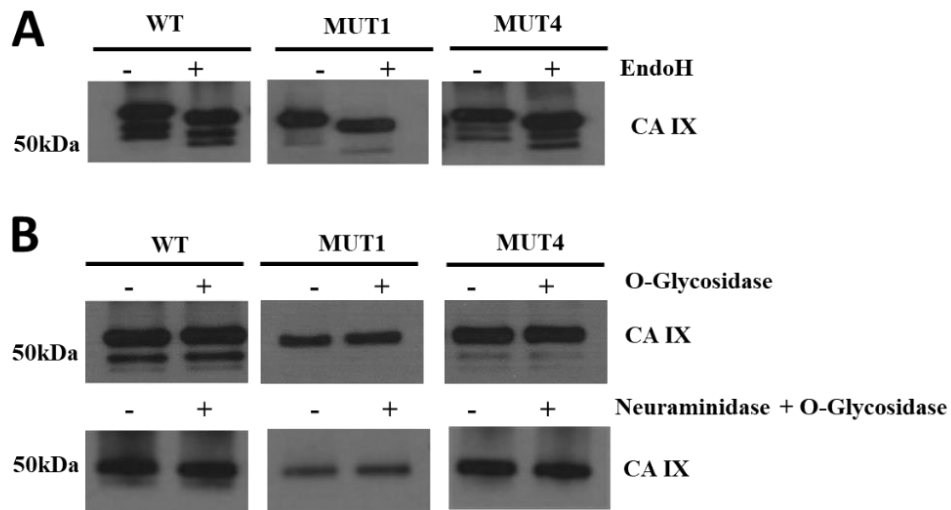


Figure 8: Glycosidase shear-sensitivity analyses of CA IX WT and its mutant forms. A) Western blot analysis of purified proteins CA IX WT, MUT1, and MUT4 digested and non-digested with EndoH. All digested samples present an electrophoretic shift when compared to undigested controls. B) Western blot analysis of purified proteins CA IX WT and mutants digested with O-glycosidase alone and combined with Neuraminidase. Undigested samples were used as negative controls. Only CA IX WT and MUT4 showed an electrophoretic shift.

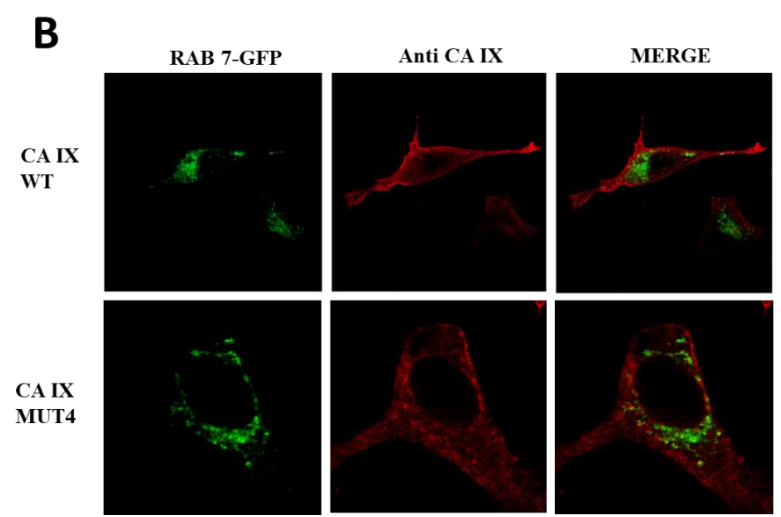
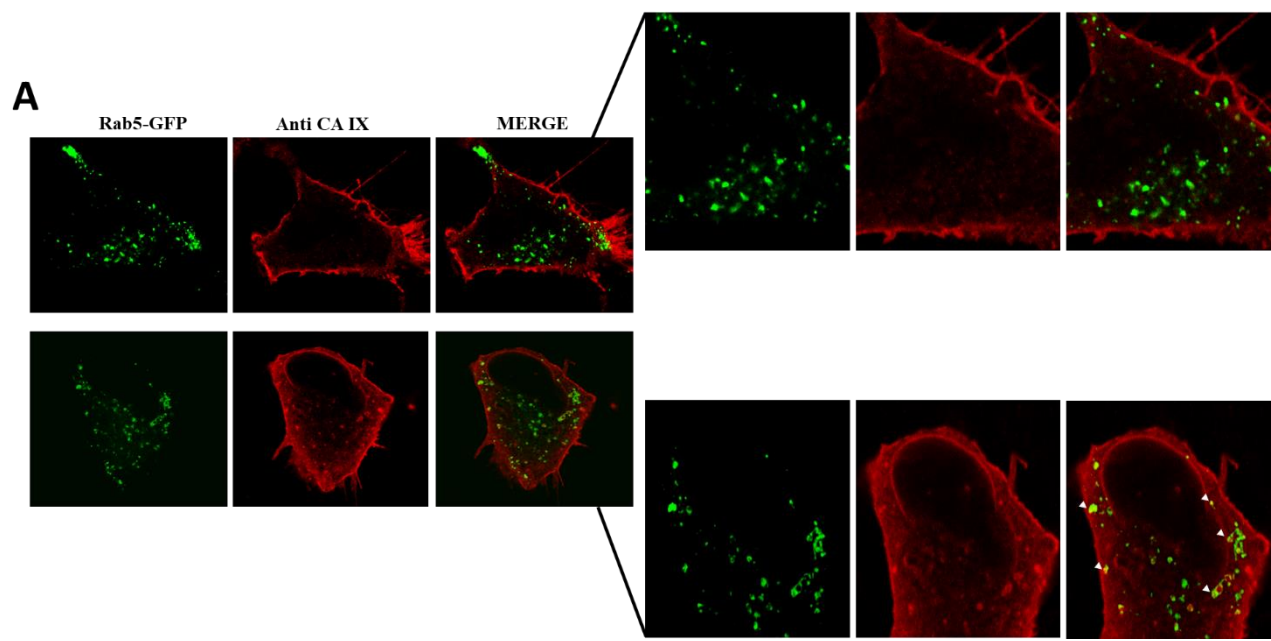
3.3 CA IX MUT4 is enriched in Rab11-containing endosomes

Having established that CA IX WT and MUT4 are able to mature through the ER and the Golgi apparatus and having observed that the MUT4 mutant is enriched in cytosolic vesicular structures, immunofluorescence experiments were performed to define the type of vesicular compartments in which MUT4 was enriched. In this regard, members of the Rab family of small GTPases, fused to EGFP, were used as vesicular markers, while CA IX proteins were detected by immunofluorescence (Figure 9). Assuming that these vesicles could be part of the endocytic circuit, we used vesicular markers EGFP-Rab5 for early endosomes, EGFP-Rab7 for late endosomes, EGFP-Rab4 for fast recycling endosomes and EGFP-Rab11 for late recycling endosomes.

Analysis of the fluorescence for EGFP-Rab5 revealed a significant amount of co-localization spots in CA IX MUT4 compared to CA IX WT, mostly due to vesicles set in proximity to the plasma membrane and the perinuclear area (Figure 9A). This could mean that MUT4 probably reaches the cell membrane and is rapidly internalized in these endosomes. Conversely, the complete lack of co-localization with Rab7 confirms that CA IX MUT4 vesicles are not intended for lysosomal degradation pathway (Figure 9B).

Further IF analysis using Rab4 vesicular marker showed no significant co-localization with both CA IX WT and MUT4 (Fig. 9C), suggesting that they are not caught in the fast-recycling endosomes toward the cell surface.

Finally, immunofluorescence analysis with Rab11 showed a weak localization with CA IX WT, and a strong localization with MUT4, especially in the vesicles scattered in the cytoplasm frequently under the cell membrane (Figure 9D), indicating that after pausing in early endosomes, the CA IX MUT4 protein could get stuck in the slow recycling endosomal trafficking.



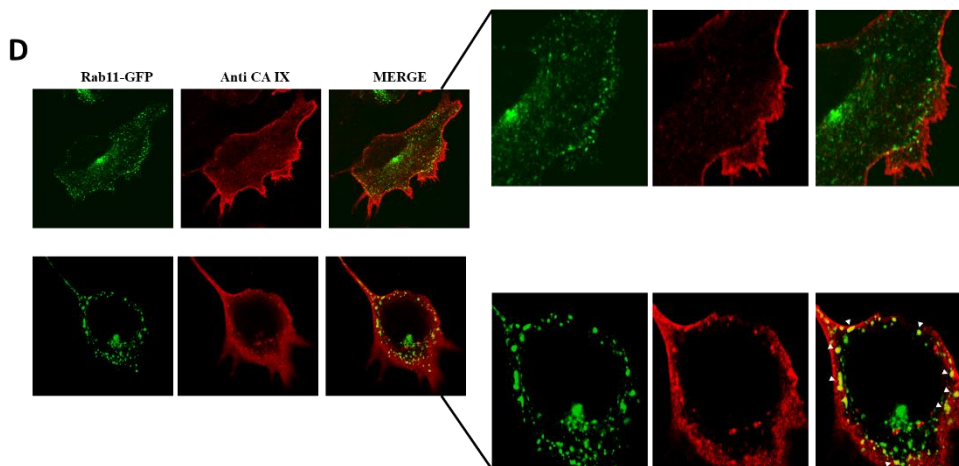
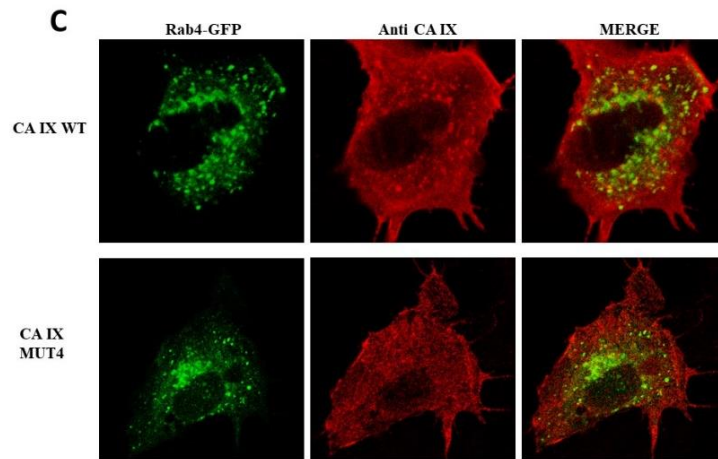


Figure 9: Co-localization analysis of CA IX WT and CA IX MUT4 with Rabs as intracellular and vesicular trafficking markers. Plasmids expressing GFP-conjugated Rabs were co-transfected with CA IX WT and MUT4. CA IX was identified by using specific polyclonal antibodies. **A)** Fluorescence analysis of Rab5-GFP (green) and CA IX (red) show co-localization spots in proximity of the plasma membrane and the perinuclear area in MUT4. **B)** Fluorescence analysis of Rab7-GFP (green) and CA IX MUT4 (red) does not show any significant co-localization between the two proteins. **C)** Immunofluorescence of Rab4-GFP (green) and CA IX (red) does not show any significant difference between CA IX WT and MUT4. **D)** Rab11-GFP (green) and CA IX (red). The images show an appreciable co-localization signal only in MUT4.

3.4 Analysis of the distribution of CA IX proteins in hypoxic conditions

Although well expressed in normoxic cells, CA IX has relevant functions in hypoxic cells where it contributes to the acidification of the extracellular space and, by acting in synergy with membrane transporters and intracellular carbonic anhydrases, to the buffering of the intracellular compartments (McDonald, Swayampakula, and Dedhar 2018; Supuran 2008).

Since CA IX mutants displayed major modifications in the cellular distribution in normoxic conditions, an IF analysis was performed to investigate the localization of CA IX mutants under hypoxic conditions (Figure 10). SH-SY5Y cells transfected with CA IX WT and subjected to hypoxia showed, as expected, a stronger membrane signal and appreciable nuclear staining, in comparison to normoxic cells. This pattern was paralleled by the presence of numerous vesicular structures in the cytoplasm. Under these conditions, an enrichment of perinuclear signals was also observed. CA IX MUT1 protein appeared to be still accumulated in the ER, which was even more pronounced by hypoxic treatments. Finally, CA IX MUT4 retained its vesicular appearance, although the vesicles seemed to be larger and denser, especially in the perinuclear region. In both mutants, plasma membrane enrichment, and nuclear localization were not discernible.

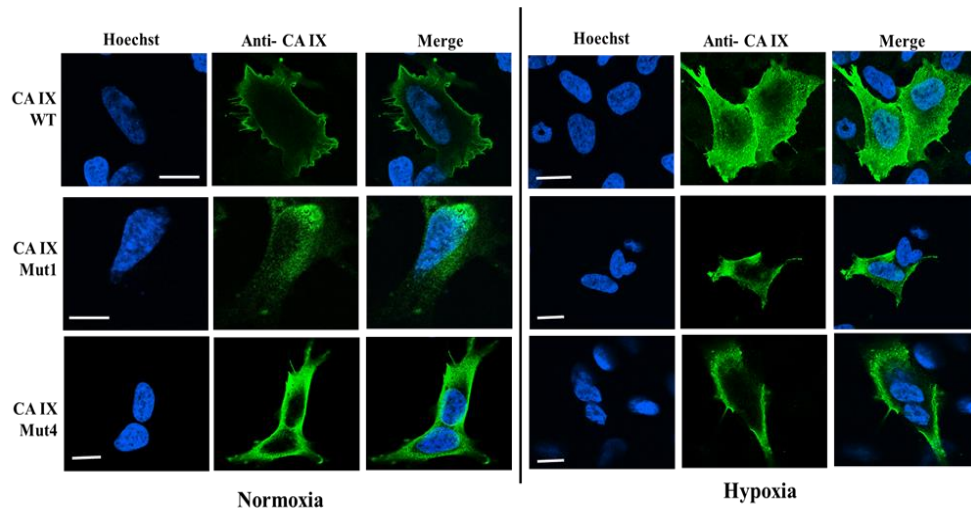


Figure 10: Analysis of CA IX subcellular distribution in Hypoxic SH-SY5Y cells. The immunofluorescence images show a nuclear enrichment in hypoxia only in CA IX WT, absent in the mutants. MUT1 still showed intense staining of the ER, widespread within the cytoplasm; MUT 4 retained its intracellular accumulations typical of vesicular structures. Also, the plasma membrane localization is absent in the mutant proteins exposed to hypoxia.

3.5 COPI-mediated retrograde trafficking from Golgi to ER is associated with the nuclear mis-translocation of CA IX WT

Accumulated evidence suggests that, in response to various extracellular stimuli, proteins traditionally described as transmembrane (i.e., RTK family members, CA IX) can change subcellular localization and compartmentalization (Brand et al. 2013; Wang and Hung 2012). These proteins are transported from the cell surface to the nucleus after endocytosis and perform multiple biological functions, including transcription regulation, cellular proliferation, tumour progression, DNA repair, and chemo- and radio-resistance. It has recently been documented that retrograde transport mediated by the COPI vesicle from Golgi to ER is involved in EGFR nuclear traffic.

To learn more about the potential mechanisms that regulate the membrane flow of CA IX to and from the ER, and to establish whether the altered cellular localization of CA IX MUT 4 was causally related to the disruption of early biosynthetic trafficking, we used brefeldin A (BFA), an antibacterial drug that inhibits *COPI* coat formation and then the transport of proteins from the ER (Bryant, Baird, and Holowka 2015; Lippincott-Schwartz et al. 1989; Misumi et al. 1986). Thus, CA IX WT and MUT4 expressing constructs were individually transfected into SHSY-5Y cells; after 48h the cells were treated with 1 µg/ml BFA for 6h. Then, their phenotype was assessed by IF analysis using CA IX and Golgin antibodies (Figure 11).

Despite the impairment of the Golgi apparatus in both treated cells, BFA-treated WT cells showed a much more robust phenotypical change, in comparison to vehicle control. Particularly, CA IX distribution in treated WT cells resembled that of untreated MUT4 cells, with a significant increase in the perinuclear signal and vesicle quantity, the hallmarks of MUT4-expressing cells. As previously observed, the double immunofluorescence staining of CAIX with the ER marker calreticulin, showed an accentuated

perinuclear signal both in cells transfected with CA IX MUT4 and treated with BFA and in control cells. Conversely, CA IX WT assumed a perinuclear localization similar to CA IX MUT4 only after the treatment with BFA, compared to the DMSO control group. Then, these experiments suggested that, in transfected cells, CA IX WT traffic may involve the intervention of COPI vesicles that mediate GOLGI -ER retrograde transport, as it happens for some members of the RTK family of membrane proteins. A possible interpretation of these results may suggest that the altered localization of the CAIX mutant could be due to inefficient GOLGI-ER retrograde transport.

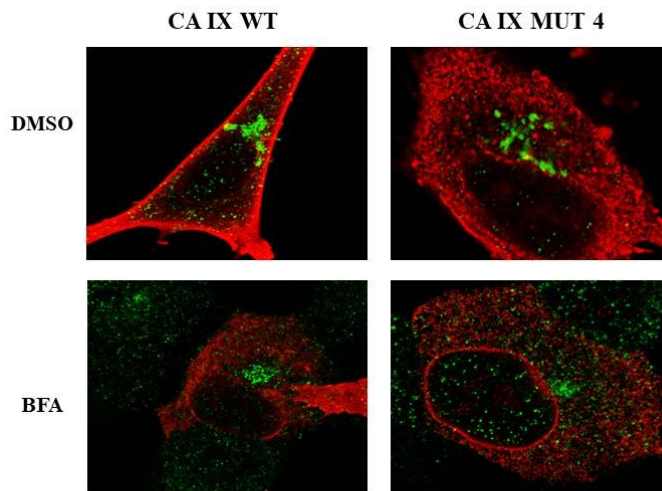


Figure 11: Effect of brefeldin treatment. Immunolocalization of golgin (green) with CA IX (red) in SHSY-5Y cells with and without BFA treatment. In CA IX WT, after BFA treatment, cells show a significant increase in the perinuclear signal and in vesicle quantity, hallmarks of MUT4 expressing cells. All images were obtained with confocal fluorescence microscopy.

3.6 CA IX subcellular localization in rat-derived primary neurons exposed to hypoxic and ischemic pre-conditioning

Although CA IX is particularly studied in cancer for its expression and activity in the hypoxic areas of tumours, truly little is known about its features in cell survival mechanisms following ischemic insults. So, after having characterized the binding/trafficking impairments of CA IX proteins in the SHSY-5Y neuroblastoma cell model, we verified the behaviour of endogenous CA IX protein in cortical neurons isolated from rats and subjected to ischemia-mimicking conditions. Rat primary cortical neurons were analysed by immunofluorescence for the neuronal marker β III-tubulin, and for CA IX expression (Figure 12). In normoxia, CA IX protein was expressed at low levels and the protein was mainly localized on the cell membrane. In neurons exposed to oxygen-glucose deprivation (OGD), a condition mimicking cerebral ischemia, a relevant increase in CAIX expression was obtained, characterized by the decoration of the plasma membrane and from the appearance of spotted nuclear enrichments. When the OGD stress was followed by reoxygenation (Rx), CA IX expression was decreased, with a localization becoming prevalently nuclear.

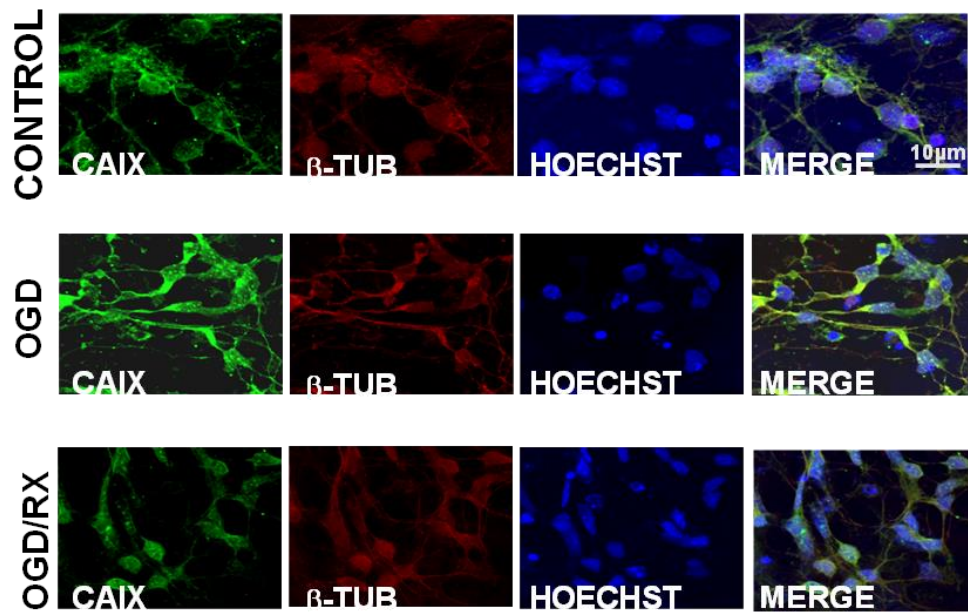


Figure 12: Expression of CA IX in rat cortical neurons exposed to OGD. Immunofluorescence analysis of CA IX (green), β -tubulin (red) and Hoechst 33342 (blue) in normal conditions, OGD and OGD/RX

3.7 Genetic ablation of CA IX in mice reveals a detrimental role in neuronal cell survival

In order to deepen the characterization of CA IX function in the experimental OGD setting, we took advantage of the availability of genetically modified mice, in which the corresponding *Car9* gene had been inactivated by homologous recombination (Gut et al. 2002); in brief, the first exon of *Car9*, which encodes for the signal peptide and for an N-terminal region of the PG domain, was interrupted by a PGK-NEO cassette of 1.8 kilobases, thus blocking the translation of the full-length protein.

Since CA IX is expected to play crucial functions in hypoxic cells, its role was investigated *ex vivo*, using mouse primary cortical neurons isolated from *Car9* WT and KO mice at E17.5, and exposed to OGD followed by Rx, to mimic the reperfusion and the oxidative stress following cerebral ischemia *in vivo*. The cell survival assay showed a significant decrease in cell viability only in WT cells, whereas the KO cells seemed not to be affected by this stress, suggesting that CA IX is detrimental to cell survival in ischemic stress, and that its absence might confer a protective role (Figure 13A).

While replicating this setting in mouse embryo fibroblasts, with the aim to account on a stable and "surrogate" model for the experimentation, without the necessity of continuous samplings, no differences were evident between wild-type and *Car9*-KO cultures of the derived mouse embryo fibroblasts. Accordingly, we cultured MEFs until their spontaneous immortalization and then we conducted hypoxic experiments with OGD/Rx and analysed cell viability. Interestingly, MEFs showed strong resistance to hypoxic stimuli and good cell survival, even at longer time points and at the highest Rx stress, so we abandoned this cellular model (Figure 13B).

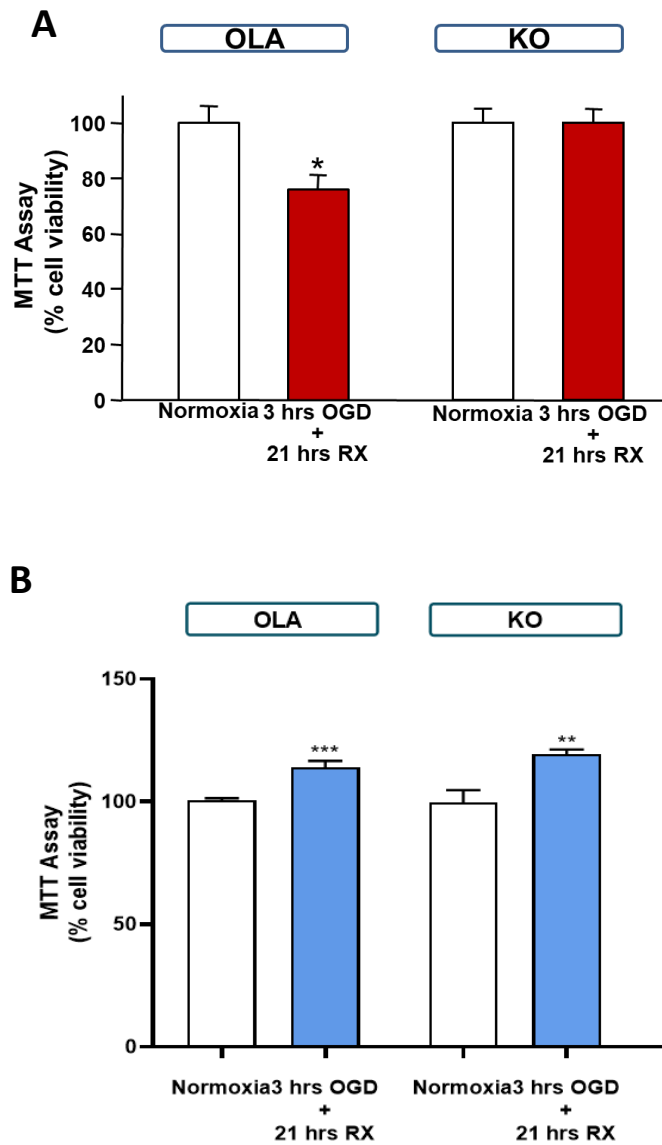


Figure 13: Viability analysis of OLA (CA IX WT) and CA IX KO mouse cells. **A)** MTT analysis of mouse primary cortical neurons exposed to 3h of OGD and 21h of RX (red). For each cell line Normoxic cells (white) were used as control. **B)** MTT analysis of mouse embryonic fibroblasts exposed to 3h of OGD and 21h of RX (blue). For each cell line Normoxic cells (white) were used as control. Statistical comparisons were performed by unpaired t-test (* $p < 0.05$; ** $p < 0.003$; *** $p < 0.001$)

3.8 CA IX inhibition by C18 phenocopies the behaviour of *Car9*-deficient cortical neurons in the OGD/RX setting

C18 represents a chemical compound that inhibits carbonic anhydrases and, due to its limited cell permeability, it may inhibit extracellularly exposed enzymes, such as CA IX (Supuran 2008). Accordingly, we characterized its role in the hypoxia/reoxygenation setting (Figure 14).

First, the toxicity of the compound was assessed in cortical neurons with a dose-escalation assay. The MTT assay showed no toxicity at 3 nM, 10 nM, and 30 nM, as cellular viability was similar to the untreated normoxic control and to the cells treated with acetazolamide, a membrane-permeant, generic inhibitor of carbonic anhydrases (Figure 14A). The cortical neurons were pre-conditioned with C18 within the selected concentration range for 16h, then exposed to 3h of OGD and after 21h of RX; next, MTT analysis was performed to assess cell viability. These cells showed a decreased viability compared to the normoxic control, whereas with increasing concentrations of C18, the viability was progressively higher and fully restored already at 10 nM concentration (Figure 14B). We then performed the C18 treatment along with the OGD, followed by RX and the achieved results were similar, since C18 was still able to restore the cellular viability, in a dose-dependent manner (Figure 14C).

Moreover, to assess whether CA IX is the main actor in this process, we pre-treated *Car9*-KO cultures of primary cortical neurons with 100 nM C18 and then exposed them to OGD/Rx, and then performed an MTT assay (Figure 15). The recovery of the viability after the treatment was observed only in CA IX WT cells, whereas no difference was observed in KO cells, indicating the specificity of CA IX inhibition.

Taken together, these results suggest that selective inhibition of extracellular carbonic anhydrases, and of CA IX in particular, play relevant

roles in OGD/RX stress and that their inhibition could lead to neuroprotection after re-oxygenation of the ischemic brain.

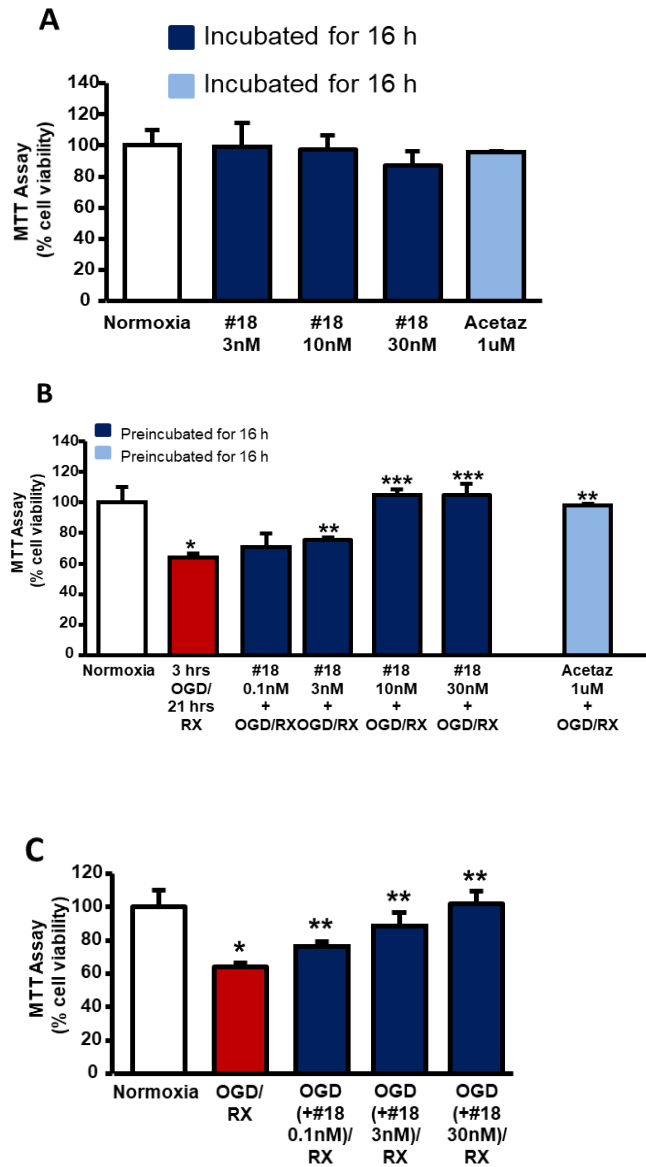


Figure 14: Viability analysis of rat cortical neurons exposed to OGD and treated with C18. **A)** Toxicology analysis of cells treated with C18 at 3nM, 10nM and 30nM (blue) and acetazolamide at 1 μ M (light blue). **B)** MTT analysis of cells preincubated for 16h with 0.1 nM, 3nM, 10nM and 30nM C18 (blue) and 1 μ M acetazolamide (light blue) or without compounds (red) and then exposed to 3h of OGD followed by 21h of RX. **C)** MTT analysis of cells exposed to OGD plus C18 at 0.1 nM, 3nM, and 30nM (blue) or no compound (red) and then exposed to RX. Normoxic cells (white) were used as control in all the assays. Statistical comparisons between groups were performed by one-way ANOVA followed by Newman-Keuls' test. (* $p < 0.05$; ** $p < 0.05$; *** $p < 0.005$).

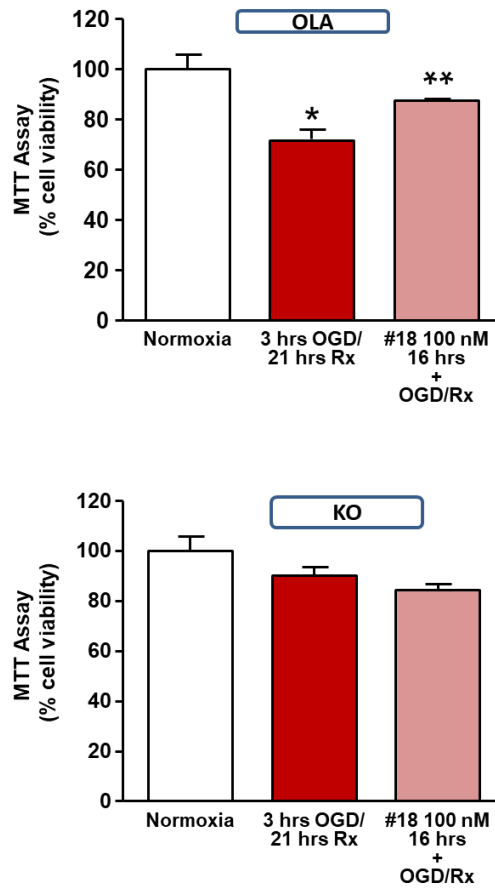


Figure 15: Viability analysis of OLA (CA IX WT) and CA IX KO primary cortical neurons exposed to OGD and treated with C18. MTT analysis of CA IX WT mouse primary cortical neurons exposed to 3h of OGD and 21h of RX (red) or preincubated for 16h with 100 nM C18 and then exposed to 3h of OGD and 21h of RX (light red). Normoxic cells (white) were used as control for OGD/Rx. For C18 preconditioning and OGD/Rx, the OGD/Rx alone was used as control. Statistical comparisons were performed by unpaired t-test (* $p < 0.05$; ** $p < 0.005$)

3.9 CA IX expression is reduced in the neurons of ischemic rats

Up to now, we established the role of CA IX in neuronal hypoxic stress and the protection given from the use of its inhibitor C18 *in vitro* in cell culture models, hereinafter we performed *ex vivo* and *in vivo* experiments in rats.

Although CA IX expression in the brain was previously reported (Gut et al. 2002), we established its localization and expression in different brain regions, to determine the most suitable regions for further analysis. So, we performed this analysis by means of immunofluorescence for co-localization of CA IX with the neuronal marker Neuregulin (NeuN). The highest expression was found in the striatum and motor cortex, followed by the cerebellum and specifically in Purkinje cells (in which it does not colocalize with NeuN). Moderate expression was found in the hippocampus and in the brainstem (Figure 16). For this, we decided to focus on the striatum and cortex to evaluate CA IX role in stroke.

To investigate whether CA IX expression was altered by ischemic insults, CA IX localization was analysed after transient middle cerebral artery occlusion (tMCAO) for 60 minutes (Figure 17). This procedure consists of the surgical occlusion of the middle cerebral artery for a limited time for one of the two brain hemispheres (ipsilateral), with the advantage of using the other hemisphere (contralateral) as an internal control. This is one of the most widely utilized models for the experimentation in rodents on focal cerebral ischemia and is aimed at mimicking the clinical scenario of early reperfusion after an ischemic infarct (Liu and McCullough 2014).

At 24h post-tMCAO, a decrease in CA IX expression was observed compared to contralateral controls, both in the cortex (Figure 17A) and in the striatum (Figure 17B). Based on the previous results of our group on CA IX role in the nucleus, we performed also co-expression analysis of CA IX with Exportin-1 (CRM1) in a similar set of samples. The immunofluorescence

analysis performed at 6h post-tMCAO showed an increased co-expression of CA IX and Exportin-1 (Figure 18).

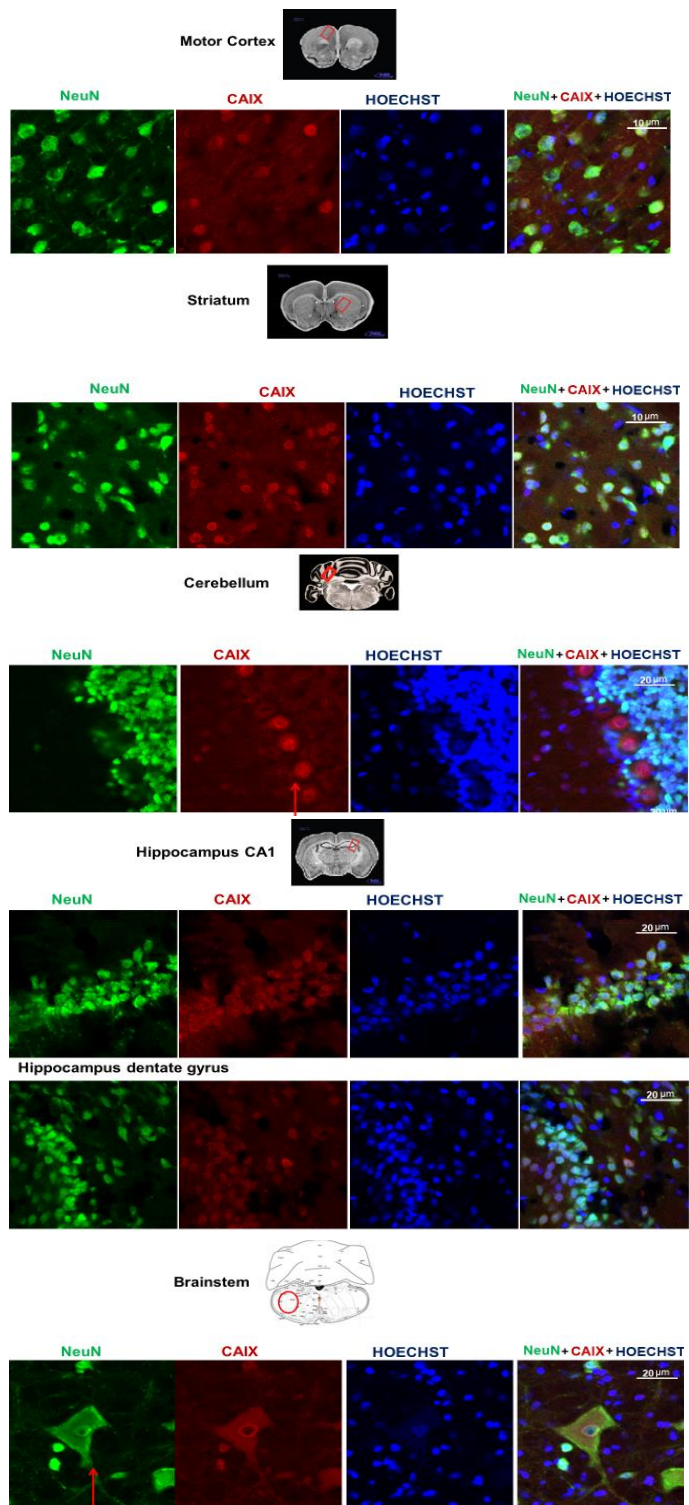


Figure 16: Immunofluorescence analysis of CA IX expression in brain regions. From top to the bottom: motor cortex, striatum, cerebellum, hippocampus, and brainstem. Neuregulin (green), CA IX (red), Hoechst 33342 (blue) and merged images are represented for each condition. The arrow in the panel shows a Purkinje cell.

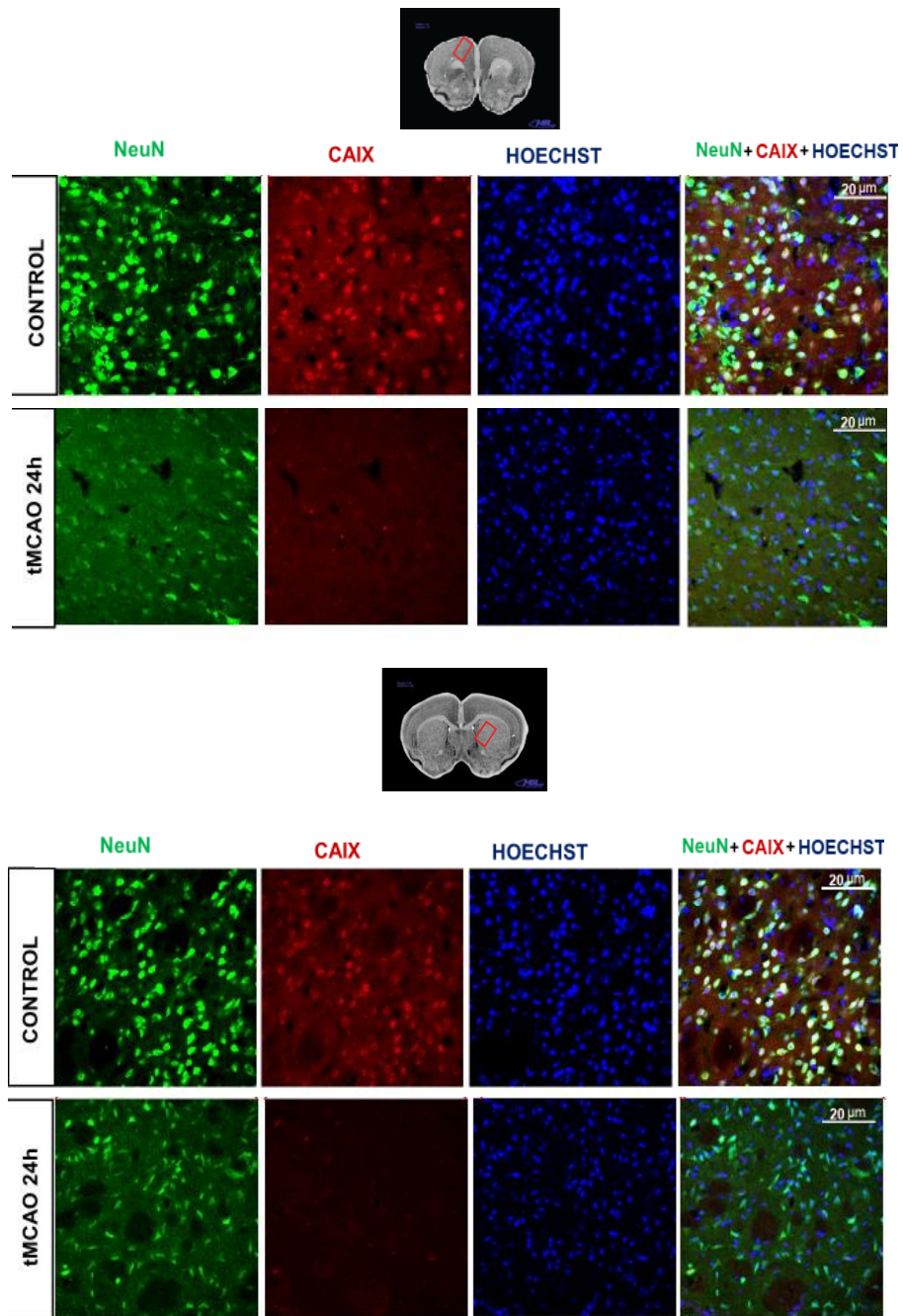


Figure 17: Immunofluorescence analysis of CA IX in rats before 60' of tMCAO and after 24h post-treatment. Neuregulin (green), CA IX (red), Hoechst 33342 (blue) and merged images are represented for each condition.

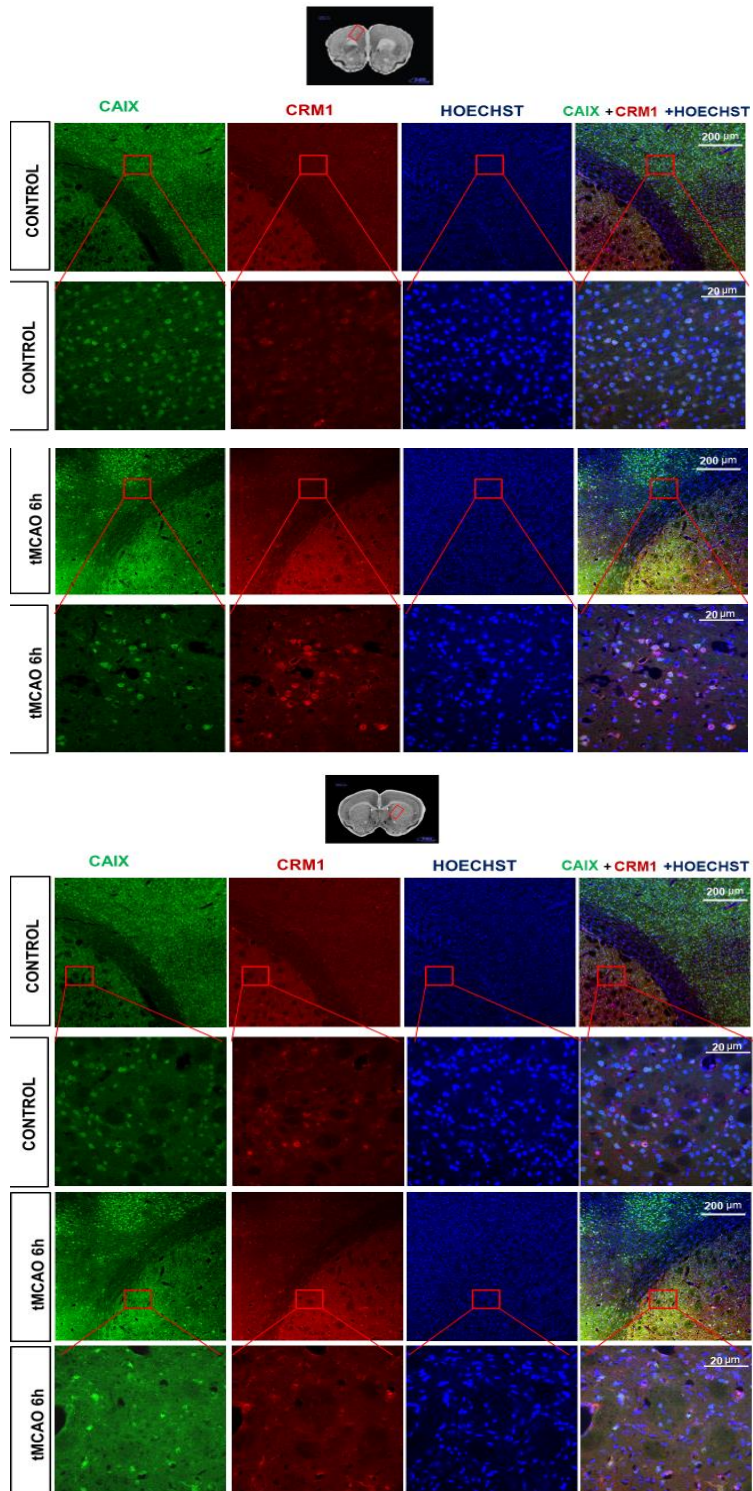


Figure 18: Co-localization analysis of CA IX (green) and CRM1 (red) in cortex and striatum of rats that underwent to 60' of tMCAO and analysed before and after 6h

3.10 CA IX inhibition is neuroprotective in rat models of ischemia

Rats treated with 5mg/kg of C18 by intracerebroventricular (ICV) administration twice (100 minutes and 3h) after tMCAO showed halved ischemic volume compared to the vehicle alone. They showed also reduced general neurological score, similar to the decrease observed in rats treated also with retigabine (an antiepileptic drug that showed efficacy in the treatment of ischemia) (Figure 19), strengthening also in this *in vivo* model the results obtained *in vitro* and *ex vivo*, which see CA IX as a relevant player of the damaging reperfusion stress observed in the ischemic brain.

We have taken a small step forward to investigate the molecular mechanisms associated with CA IX function in the ischemic insults, performing molecular analysis of protein levels in striatum and cortex samples from rats treated with C18 and exposed to tMCAO (Figure 20). In these rats, we found a decrease of CA IX and CA II protein expression in the ipsilateral brain, compared to contralateral control. We analysed the main proteins for the representative pathways involved in ischemia: inflammation (NFkB), apoptosis (Cl-Cas3), oxidative stress (SOD1), and neurotoxicity (nNOS). They all showed the same downregulation in both the ipsilateral cortex and striatum compared to the corresponding controls. On the contrary, CA XII seemed to put in action a compensatory mechanism, with an increased expression both in the cortex and in the striatum. BiP remained constant in all the samples, indicating that reticular stress was not involved in the process. B-actin was used for normalization.

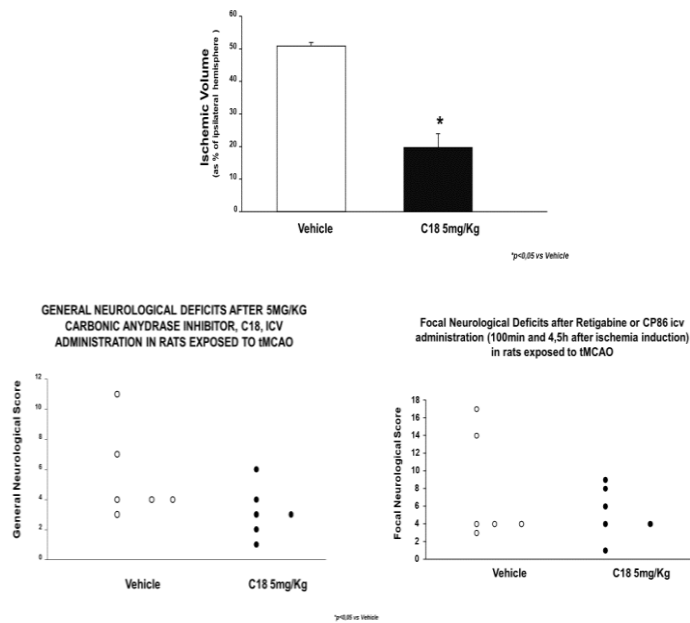


Figure 19: Ischemic volume and neurological score of rats treated with 5mg/kg of C18 and undergone to tMCAO for 60’. Ischemic volume is represented as % of the ipsilateral hemisphere. Left: Neurological score of rats treated with C18 alone and underwent to tMCAO. Right: Neurological score of rats treated with C18 and after retigabine administration.

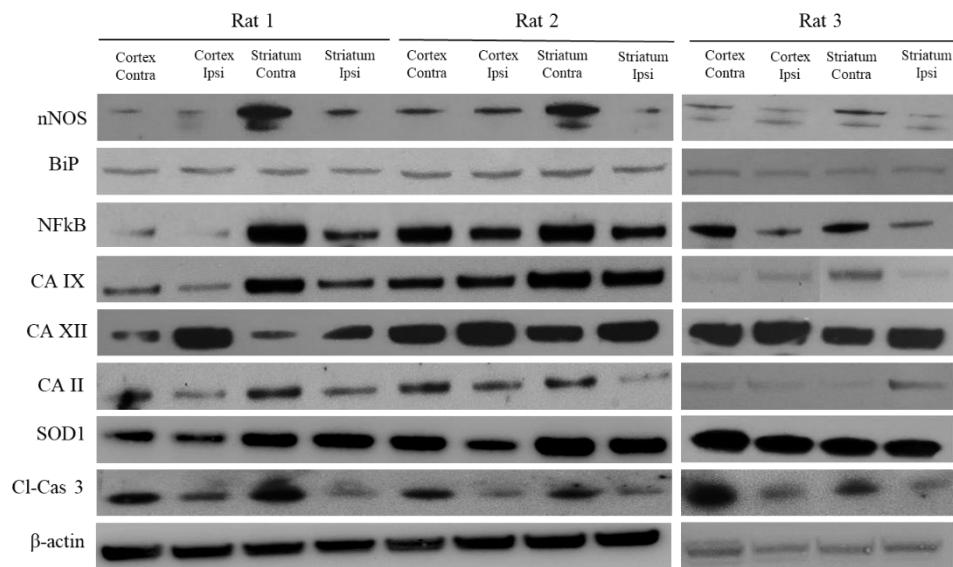


Figure 20: Protein analysis of CAs, inflammation, apoptosis, oxidative stress markers. For each rat treated with C18 the contralateral (contra) and the ipsilateral (ipsi) samples for both cortex and striatum are represented. The analysed proteins are listed based on their molecular weight: nNOS, BiP, NFkB, CA IX, CA XII, CA II, SOD1, Cleaved Caspase 3 and B-actin used as control.

4. Discussion

The increase in co-localization and the well-established body of knowledge acquired on CA IX interactions with proteins of the nucleocytoplasmic shuttling and its nuclear localization prompted me to focus on mutagenesis of CA IX in a neuroblastoma-derived cellular model, namely the SH-SY5Y cell line. Indeed, beyond the expression on the cell membrane, several cells express CA IX in the nucleus, where its function may contribute to transcription modulation of 47S rRNA precursor genes. The identification of the whole machinery of nuclear import/export as the main component of its interactome and of nuclear localization sequences (NES and NLS) in the C-terminal of the protein, provides a strong rationale for the nuclear localization of CA IX.

Intriguingly, the NES sequence sits in the transmembrane alpha helix of CA IX in its membrane-bound topology, while the NLS is part of the short intra-cytosolic domain. The region encompassing both nuclear trafficking sequences has been identified as the minimal portion of the protein required for interaction with importins and exportins (Buanne et al. 2013), as well as for binding to CAND1, model of the binding with interactors (Buonanno et al. 2017). Yet, the mechanisms ensuring the nuclear translocation of CA IX have not been clarified. With the purpose of elucidating the subcellular trafficking of CA IX, we exploited the mutants contributing to the latter evidence, designed on the basis of molecular modelling. These mutants did not simply cause a loss of interaction with endogenous CA IX ligands but demonstrated also a very peculiar subcellular localization, based on the profound modifications introduced in key regions of the protein.

The modification of the transmembrane alpha helix, containing the NES sequence, characteristic of CA IX MUT1 comes with the most severe phenotype. It is clearly trapped within the ER, where it acquires the N-

glycosylation correctly, but it fails to reach the Golgi apparatus, lacking the typical O-glycosylation acquired through the Golgi transit and therefore, does not reach the membrane. Entangled in the ER, this mutant induces unfolded protein response, with the increase of its marker GRP78. On the contrary, the CA IX MUT4 protein is competent for the transit through the secretory pathway and partially reaches the plasma membrane, but it is incompetent for membrane stabilization, showing rapid internalization and characteristic vesicular localization, particularly in endosomes labelled by Rab5 (early) and Rab11 (late recycling).

Regarding nuclear localization, both mutants showed the inability to localize in the nucleus, even in the presence of the nuclear export inhibitor LMB. Although it has been described that hypoxia increases the nuclear mobilization of CA IX (Buanne et al. 2013; Sasso et al. 2015), the hypoxic stimulation caused nuclear translocation of neither of the two mutants, whereas the wild-type CA IX correctly increased its representation in both plasma membrane and in the nucleus. Last but not least, the blockade of Golgi-ER trafficking inflicted by brefeldin A treatment displayed the nuclear mis-translocation of CA IX WT protein too, with a subcellular localization resembling the one of MUT4 in normal condition, whereas MUT4 showed evident perinuclear accumulation.

Increasing evidence suggests that proteins traditionally described as transmembrane, as members of the RTK family, can modify their subcellular localization through retrograde Golgi-ER pathway in response to extracellular stimuli to exert additional biological function, indicating that CA IX does not stand alone as a membrane protein with unusual nuclear trafficking and that this localization might follow a similar route. Indeed, a reasonable interpretation of these results is that CA IX requires to transit within the secretory and endocytic pathways in order to translocate through the nucleus. This is supported by our model in which mutant CA IX proteins are stuck into

ER (MUT1) and endocytic (MUT4) subcellular compartments and are unable to reach the nuclear compartment.

The human CA IX is canonically described as a hypoxia-induced transmembrane protein belonging to α -CAs enzyme family. CA IX has a crucial role in pH regulation, especially in hypoxic cells and acts in a concerted action with intracellular CAs, by buffering intracellular acidosis induced by hypoxia, which results in extracellular pH acidification. This strategy is usually implemented by tumour cells to avoid immune surveillance and to promote invasiveness and resistance to chemo- and radiotherapy. In fact, CA IX is a major effector of HIF-1 α activity in the metabolic adaptation of hypoxic tumours, the so-called Warburg effect and is linked to a worse prognosis. In normal tissues, CA IX expression is tightly controlled by oxygen levels, almost undetectable under normoxic condition, and heavily induced by hypoxia.

Besides this well-known membrane role in tumorigenicity, CA IX is possibly involved in additional physio-pathological processes connected with pH and CO₂ homeostasis. Among these, it is worth mentioning cerebral ischemia. Cerebral acidosis, following ischemic insult, causes neuronal injury by generating free radicals affecting glutamate uptake and causing neuronal apoptosis. Despite the advances in the comprehension of the pathophysiology of cerebrovascular injury, outright stroke treatment continues to represent an important unmet medical need and research is struggling to identify adequate therapeutic and preventive measures.

Due to CAs role in pH and body volume regulation, it has been assumed that its targeting with inhibitors could be used to manage ischemia, in synergy with CAIs function as diuretics. Indeed, the putative protective effect of carbonic anhydrase inhibition in brain ischemia was previously investigated (Bulli et al. 2021; Di Cesare Mannelli et al. 2016). In these

works, CAIs re-established the architecture of the ischemic cortex and striatum, counteracted neuronal and astrocyte loss, and reduced microglial activation. However, they only hypothesized the relevance of the role of membrane bound CAs, but they do not provide a clear demonstration. Therefore, our work aimed to characterize the potential involvement of CA IX in ischemic damage *in vitro* and *in vivo*. To this aim, we exploited loss-of-function strategies, targeting CA IX through mutagenesis, genetic knock-out models, and enzymatic inhibition.

Actually, CA IX subcellular distribution varied in rat-derived primary neurons exposed to OGD/RX, the *in vitro* substitute for ischemic insult, with increases on plasma membrane only after OGD, and exacerbation of the nuclear localization after OGD/RX; accordingly, it can be postulated that CA IX trafficking is associated to cellular responses to these stressful conditions. Namely, the nuclear accumulation observed for CA IX and its ligand CRM1 after OGD/RX recalls the involvement of their complex in the nucleolar stress events, associated to a general translation attenuation following hypoxic exposure (Sasso et al., 2015).

The weak phenotypes which characterize *Car9* knock-out mice suggest that more relevant phenotypes might emerge under stressful conditions, such as ischemia. The *Car9*^{-/-} mice allowed us to perform *in vitro* studies of both neuronal and non-neuronal cell cultures. Interestingly, mice-derived cell cultures revealed not only the harmful role of CA IX for cell survival, but also that this phenomenon can be selectively modelled in neurons and not in other cell types (i.e., stabilized fibroblasts), suggesting a potential tissue-specificity of the generated evidence.

Taking into account that in these years a lot of efforts have been spent to discover and characterize CAIs, in particular for the tumours overexpressing the prognosis marker CA IX, and that genetic inhibition may

only provide proof of concept evidence for the opportunity to inhibit CA IX in ischemic stroke, we shifted toward the evaluation of CA IX enzyme inhibition. We focused on the availability of the cell-impermeant sulphonamide compound C18 (Supuran 2008). In virtue of its positive charge, it is not able to cross the cellular membrane and therefore was described for the first time as a putative selective inhibitor of CA IX and CA XII. Remarkably, the behaviour of *Car9*^{-/-} cortical neurons was phenocopied by C18 inhibition in OGD/RX cortical neurons and directly proportional to the dosage and only in *Car9*^{+/+} cells, indicating that CA IX is a main contributor to the observed increased neuronal survival.

We then moved on to *in vivo* experiments in rats exposed to tMCAO. As a starting point, we established the striatum and the motor cortex as the most suitable regions for the analysis, since they expressed CA IX at higher levels and therefore would probably be mostly affected by its presence. In both regions, CA IX expression decreased at 24h post-tMCAO and its colocalization with CRM1, which belongs to the family of exportins, resulted increased. Taken together, these results not only suggest that the selective inhibition of extracellular carbonic anhydrases play relevant roles in OGD/RX stress and that their inhibition could lead to neuroprotection after of ischemic brain re-oxygenation, but also that CA IX nuclear function could also mediate its detrimental role in ischemic insult.

Furthermore, extracellular inhibition of carbonic anhydrases resulted neuroprotective *in vivo* in the rat models of ischemia, showing a better phenotype measured as reduction of ischemic volume and neurological score. Protein analysis in the same setting showed interesting though unexpected results. Indeed, we noted an inexplicably reduction in the main proteins for representative pathways involved in ischemia such as inflammation (NFkB), apoptosis (Cl-Cas3), oxidative stress (SOD1), and neurotoxicity (nNOS), which could be explained either as a CA IX-dependent mechanism or as

obscured by the damaged tissue. In countertendency, the only protein that showed overexpression was CA XII, which is possibly the result of a compensatory mechanism. Surely, the acquired evidence is at a preliminary stage; a deeper characterization of the mechanisms involved in the neuroprotective function of CA IX inhibition, and the potential contribution by other CAs, but these findings could pave the way to the preclinical characterization of CA IX inhibition in stroke.

5. Conclusions

The experimental exploitation of the three loss-of-function strategies reported in this thesis allowed us to deepen the knowledge of CA IX subcellular trafficking and its contribution to hypoxic insults, *in vitro* and *in vivo*.

First, we characterized CA IX subcellular trafficking through the inactivation of its binding ability with intracellular ligands, by site-directed mutagenesis. The analysed mutants were shown to be unable to stably reside on the plasma membrane and to reach the nucleus; their nuclear translocation was not observed even with experiments aimed at stressing this condition. In addition, the blockade of ER-Golgi trafficking showed impairment also in the nuclear mobilization of the wild-type form. These experiments allowed us to hypothesize the route to the nucleus of this transmembrane protein, which probably requires its normal transit through the secretory pathway and the following intracellular recycling.

Secondly, we uncovered a relevant role of CA IX in ischemia through mouse models of genetic ablation. We focused on both neuronal and non-neuronal Car9 *-/-* derived cell cultures. In OGD experiments followed by Rx, only the neuronal model highlighted the importance of CA IX for cell survival, indicating the potential tissue specificity of its detrimental effect.

Third, we explored the CA IX role in brain ischemia and the potential beneficial effect of its enzymatic inhibition in rat models. The induction of cerebral ischemia *in vivo* showed a decrease of CA IX neuronal expression and enhanced co-localization with exportins. The use of C18, a sulphonamide compound unable to cross the plasma membrane showed satisfactory results both *in vitro* and *in vivo*. *In vitro*, it restored cell viability in rat-derived neurons, in direct proportionality to the posology. *In vivo*, it improved mice recovery after the induction of ischemia, reducing the ischemic volume and the neurological score. These results suggest that the inhibition of CA IX

plays a fundamental role in ischemic stress and that its inhibition might be neuroprotective, but also that CA IX detrimental role could be associated with its nuclear function.

Although we provided better evidence for both CA IX nuclear translocation and for its neuroprotection after the ischemic insult, further experiments will be required to characterize in greater details the molecular mechanisms underlying these processes.

6. Materials and methods

Cell lines

SH-SY5Y human neuroblastoma cell line was purchased from ATCC. Cells were cultured in standard conditions using DMEM (Sigma) complemented with 15% FBS, 2% glutamine, 1% penicillin/streptomycin at 37 °C in 5% CO₂ humidified atmosphere.

Rat primary cortical neurons were taken from E17.5 Wistar rat embryos (Charles River). Dissection and dissociation were conducted in Ca²⁺ and Mg²⁺-free PBS with 30 mM glucose. Tissues were incubated with papain at 37°C for 10 min and dissociated by trituration in Earle's balanced salt solution (EBSS) containing 0.16 U/mL DNase, 10 mg/mL BSA 10 mg/mL, and 10 mg/mL ovomucoid. Neurons were thus plated on Petri dishes treated with poly-d-lysine 20 µg/mL and were grown in DMEM/F12 with glucose, 5% FBS and 5% horse serum, 2 mM glutamine, 50 U/mL penicillin and 50 µg/mL streptomycin. To prevent non-neuronal cell growth 10 µM arabinoside-C was added within 48h. Neurons were cultured at 37°C in a humidified 5% CO₂ atmosphere and used after 7–10 days of culture (Sisalli et al. 2014).

Using the same procedure, mouse primary cortical neurons were collected from E17.5 C57B6 mice WT (Ola) and CA IX KO brains.

Mouse embryonic fibroblasts (MEFs) were taken from the same E17.5 C57B6 mice WT (Ola) and CA IX KO, using the embryos from which the brain and abdominal organs were removed as described here (Conner 2001). Tissues were minced and dissociated with trypsin-EDTA 0.25% for 10 minutes. Large pieces of tissues were removed with sedimentation and then cells were centrifuged at 1000 RPM for 5 minutes, resuspended and put in culture. MEFs were cultured using DMEM supplemented with 10% FBS, 1% glutamine, 2% penicillin/streptomycin, 1% MEM Non-Essential Amino

Acids and 20mM HEPES at 37 °C in 5% CO₂ humidified atmosphere until their spontaneous immortalization.

Treatments

Vectors encoding for CA IX WT and mutant proteins have been previously described (Buanne et al. 2013; Buonanno et al. 2017). Transient transfections of these plasmids were performed on SH-SY5Y cells at 90% confluence using TransFectin Lipid Reagent (Bio-Rad) and cells were incubated for 48 hours at 37 °C in humidified air with 5% CO₂, cell medium was renewed after 24 hours.

Leptomycin B treatment was performed 24 hours post-transfection. Cells were incubated for 5 hours with leptomycin B (LMB; Sigma) at a final concentration of 20 ng/mL, or with 70% methanol as negative control.

Brefeldin A (B5936- Sigma-Aldrich) was used in culturing cells for 6 h with a final concentration of 1µg/mL.

Hypoxia was performed in a hypoxia incubator chamber (STEMCELL Technologies), blowing 95% N₂ and 5% CO₂ gas for 6 minutes and repeating the same treatment after 30 minutes to expel all the O₂ from the chamber. Hypoxia lasted for 6h. Cells incubated for the same time at 37 °C in humidified air with 5% CO₂ were used as normoxia control (Sasso et al. 2015).

Oxygen and glucose deprivation was performed for 3h in the hypoxic chamber and using a medium containing NaCl 116 mM, KCl 5.4 mM, MgSO₄ 0.8 mM, NaHCO₃ 26.2 mM, NaH₂PO₄ 1 mM, CaCl₂ 1.8 mM, glycine 0.01 mM. After the incubation, cells were removed from the hypoxic chamber and the glucose-free medium was replaced with the usual complete medium. Thus, cells were reoxygenated by returning neurons to normoxic conditions (5% CO₂ and 95% air) for 24 h (Sisalli et al. 2014).

To inhibit CA IX, C18 compound was dissolved in DMSO 20% - PBS and used at the following concentrations: 3nM, 10nM and 30nM. Acetazolamide was dissolved in DMSO 20%-PBS and used at the final concentration of 1mM. DMSO 20%-PBS was used as negative control. CA IX inhibitor was kindly provided by Giuseppina de Simone (Institute of biostructure and bioimaging, CNR, Naples).

Cell viability assay

PrestoBlue Cell Viability Reagent A13261 (Invitrogen) was used to perform cell viability assay according to manufacturer's instruction. In brief, cells were seeded in black 96-well with clear and flat bottom at least 24h before treatment or assays and incubated at 37 °C in humidified air with 5% CO₂. Then PrestoBlue was added at a final concentration of 1x directly in the cell-containing medium and incubated for 45 minutes in the dark at 37 °C in humidified air with 5% CO₂. Fluorescence was read using an excitation wavelength of 560 nm and an emission of 590 nm with EnSpire multimode plate reader (PerkinElmer).

Cell lysis and western blotting

SH-SY5Y cells were rinsed with PBS, harvested, and lysed with 50 mM Tris-HCl, 150 mM NaCl, 0.5% Triton X-100, 10% glycerol, 50 mM NaF, 1 mM Na₃VO₄, 1 mM DTT cold buffer containing a cocktail of proteases inhibitors (Sigma Aldrich).

Brain tissues were collected from euthanized rats as reported below. Contralateral and ipsilateral striatum and cortex were removed, weighted, and cryopreserved at -20°C for protein analysis. Proteins were lysed with a buffer containing 20 mM HEPES pH 7.4, 1mM NaN₃, 1% Triton X-100, 200 μM Na₃VO₄, 50 mM NaF, and a cocktail of proteases inhibitors (Sigma Aldrich).

Briefly, in a glass Dounce were added 6 volumes (w/v) of ice-cold lysis buffer, and manual homogenization of the tissues was conducted until the compound was homogeneous.

Lysates were clarified by centrifugation at 12.000 x g for 20 min at 4°C and collected and quantified with BioRad Protein Assay, based on the Bradford method, using a standard curve of BSA and according to manufacturer's instructions.

Protein samples (30 ug each) were resolved by SDS-PAGE, on NuPAGE Bis-Tris 4–12% gradient gels (Invitrogen), transferred onto a PVDF membrane (Millipore) and blocked with 5% non-fat Milk.

Target proteins were detected using the following primary antibodies: monoclonal mouse anti-CA IX M75 (1:300); mouse monoclonal anti-GRP78 (1:100) (Santa Cruz Biotechnology); polyclonal rabbit anti-BiP #3183 (1:1000) (Cell Signalling technologies); polyclonal rabbit anti-Cleaved Caspase-3 (Asp175) #9661 (Cell Signalling technologies); monoclonal rabbit anti-nNOS #4231 (C7D7) (1:1000) (Cell Signalling technologies); monoclonal rabbit anti-SOD1 (E4G1H) #37385 (1:1000) (Cell Signalling technologies); mouse monoclonal anti-CA II (G-2) sc-48351 (1:1000) (Santa Cruz Biotechnology); rabbit monoclonal NFkB p65 (D14E12) #8242 (1:1000) (Cell Signalling technologies); mouse monoclonal anti-CA XII (A-3) sc-374313 (1:1000) (Santa Cruz Biotechnology); rabbit polyclonal anti-CA IX (PA5-77885) (1:1000) (Invitrogen), mouse monoclonal anti-beta actin sc-81178 (1:2000) (Santa Cruz Biotechnology). Then, the respective peroxidase-conjugated anti-mouse secondary antibody (1:10000) (Santa Cruz Biotechnology) or anti-rabbit secondary antibody (1:5000) (Santa Cruz Biotechnology) was used. Immunoreactive bands were detected by ECL (Amersham) and acquired with Chemi Doc Imaging System (BioRad) or with X-ray films (Fujifilm).

Immunofluorescence analysis

SH-SY5Y cells were plated on glass slides and fixed for 20 min with 3% paraformaldehyde in PBS after 48h from transfection and rinsed three times with PBS. Rat primary cortical neurons were fixed at room temperature in 4% (w/v) paraformaldehyde for 20 minutes and washed 3 times with PBS. Brain sections were incubated in proteinase K buffer containing 1 M Tris-HCl (pH 7.4), 0.5 M EDTA, 5 M NaCl, and proteinase K (15 µg/mL) in RNase-free water at 37°C for 10 min, rinsed three times for 3 minutes in PBS. Cells were permeabilized with 0.3% Triton X-100 in PBS for 4 min and rinsed. To reduce nonspecific signal, SH-SY5Y cells, and rat primary cortical neurons were treated with 1% BSA-PBS for 30 min, whereas brain sections were blocked with a solution containing 2% sheep serum and 1% BSA in PBS with 0.1% Tween-20 for 15 min at room temperature.

Cells were then incubated for 2h with specific primary antibodies in humidified chamber. In the various experiments were used: anti-CA IX VII/20 (1:80) mouse monoclonal; anti-CA9 H-120 (1:100) (Santa Cruz Biotechnology) rabbit polyclonal; anti-Calreticulin (1:120) rabbit polyclonal; anti-Golgin (1:120) mouse monoclonal. Rat primary cortical neurons were incubated with anti-CA9 H-120 (1:100) (Santa Cruz Biotechnology) rabbit polyclonal and β III tubulin (1:200) (Santa Cruz Biotechnology). After washing three times for 3 minutes in PBS, brain sections were incubated with the following primary antibodies in blocking solution: anti-NeuN (1:200) (Elabscience), anti-CA9 H-120 (1:100) (Santa Cruz Biotechnology) rabbit polyclonal and mouse monoclonal anti-CRM1 (C-1) sc-74454 (Santa Cruz Biotechnology) overnight. To visualize the targeted proteins by fluorescence, after 3 washes with PBS, samples were incubated in a humidified chamber for 1h (cells) and 2h (tissues) with secondary antibodies Alexa-488-conjugated donkey anti-mouse, Alexa-488-conjugated donkey anti-rabbit (1:200) (Jackson Laboratories), Alexa-546-conjugated donkey anti-mouse and Alexa-546-conjugated donkey anti-rabbit (1:200) (Jackson Laboratories). Finally, cell nuclei were marked with Hoechst staining (1:3000) for 20 min

and washed two times with PBS. Cells were mounted onto microscope slides with Glycerol/PBS 1:1; sections were mounted onto slides using Fluoromount aqueous mounting medium (Sigma) and both were air-dried and stored in a dark room. Fluorescence was observed at confocal microscope (Zeiss LM510) under the supervision of Prof. Corrado Garbi (Department of Biology and Molecular and Cellular Pathology, Federico II University of Naples) or using a Zeiss LSM 700 laser scanning confocal microscope.

For the co-localization studies of CA IX, its mutants, and vesicular Rab markers using immunofluorescence we used plasmids driving the expression of Rabs conjugated with EGFP kindly provided by Prof. Simona Paladino (Department of Molecular Medicine and Medical Biotechnology, Federico II University of Naples) and Chiara Zurzolo (Pasteur Institute, Paris).

Glycosidase shear-sensitivity analysis

Glycosidase shear-sensitivity analysis were conducted on CA IX WT, CA IX MUT1, and CA IX MUT 4 purified proteins using New England BioLabs reagents according to manufacturer instructions. Samples (1 µg) were firstly denatured with Glycoprotein Denaturing Buffer (0.5% SDS, 40 mM DTT) at 100°C for 10 min. For N-glycosidase analysis, GlycoBuffer 3 (50 mM Sodium Acetate, pH 6.0) and EndoH enzyme were added and incubated for 2 h at 37°C. For O-glycosidase analysis GlycoBuffer 2 (50 mM Sodium Phosphate, pH 7.5), 1% NP40, Neuraminidase, and O-Glycosidase were added to denatured samples and incubated at 37°C for 4 h. Digested samples were visualized on 11% SDS-PAGE followed by western blotting using anti-CA IX M75 as primary antibody and anti-mouse as the secondary antibody.

Animals

For the present study were used *Mus musculus Car9* Knock-out in C57B6 genetic background and Male Sprague Dawley rats. Animal studies were performed in collaboration with Professor Agnese Secondo from the Department of Neuroscience and Reproductive and Odontostomatological Sciences, Federico II University of Naples. Animals with inactivating mutation of the *Car9* gene have previously been generated and described (Gut et al. 2002), and were firstly made available by Prof. Seppo Parkkila (Faculty of Medicine and Life Sciences, University of Tampere, Finland). The animals included in this study were housed using procedures as described in the Jackson Lab Resource Handbook. Experiments were performed according to the international guidelines for animal research and approved by the Animal Care Committee of “Federico II” University of Naples, Italy and Ministry of Health, Italy. For any surgical or invasive procedure, animals were anesthetized using sevoflurane at 3.5% (Medical Oxygen Concentrator LFY-I-5A) in a mixture with oxygen. Euthanasia was performed by an overdose of sevoflurane at 6h or at 24h post- tMCAO to evaluate infarct volume or protein expression.

Transient middle cerebral artery occlusion (tMCAO) and drug administration

In vivo experiments were made in collaboration with Prof. Giuseppe Pignataro (Department of Neuroscience and Reproductive and Odontostomatological Sciences, Federico II University of Naples) and his group. Transient focal ischemia was induced in anesthetized rats by middle cerebral artery occlusion for 60 minutes (Pignataro et al. 2011). In brief, under an operating stereomicroscope Nikon SMZ800 (Nikon Instruments), a 5-0 surgical monofilament nylon suture was introduced through the right external carotid artery into the circle of Willis for 19 mm to reach the origin of the

middle cerebral artery (MCA), thus blocking blood flow through the artery. To confirm the achievement of ischemia, cerebral blood flow was monitored through a disposable microtip fiber optic probe (diameter 0.5 mm) connected through a primary probe to a laser Doppler computerized main unit (PF5001) and analysed using PSW Perisoft 2.5.

The C18 compound (5mg/Kg) was administered ivc (intracerebroventricularly) twice: 100 minutes and 3h after ischemia induction in rats exposed to tMCAO.

Neurological score

Neurological scores were evaluated before euthanasia by Prof. Giuseppe Pignataro's group, according to two scales: the general neurological scale and the focal neurological scale. For the general neurological score, were measured the conditions of the hair, position of ears, conditions of the eyes, posture, spontaneous activity on the bench, and the presence of epileptic behaviour. The obtained scores were then summed to have a general neurological score, ranging between 0 and 28 depending on the severity of signs. For the focal neurological score were considered the symmetry of the body, gait, the ability to climb, the presence of circling behaviour, front limb asymmetry, compulsory circling, and whisker response. The focal neurological score was then obtained by the addition of each component (Pignataro et al. 2007).

Evaluation of the infarct volume

The evaluation of the infarct volume was performed by Prof. Giuseppe Pignataro's group as described in their previous work (Pignataro et al. 2011).

Before euthanasia animals were perfused transcardially under deep anaesthesia with 0,9% saline solution, followed by 4% paraformaldehyde (Sigma) in phosphate-buffered saline. The brains were removed and postfixed overnight at + 4 C° and cryoprotected in 30% sucrose phosphate buffer saline. Frozen brains were sectioned with a sliding cryostat at 40 µm thickness and Nissl staining was performed. Infarct volume was calculated by summing the infarction areas of all sections and by multiplying the total by slice thickness. To avoid the bias caused by the presence of the oedema, the infarct volume was expressed as a percentage of the infarct volume of the total ipsilateral hemispheric volume.

Statistical analysis

Statistical comparisons between groups were performed by unpaired t-test or by one-way ANOVA followed by Newman-Keuls' test.

7. Bibliography

Article in a journal

- Aebi, M. 2013. 'N-linked protein glycosylation in the ER', *Biochim Biophys Acta*, 1833: 2430-7.
- Alterio, V., M. Hilvo, A. Di Fiore, C. T. Supuran, P. Pan, S. Parkkila, A. Scaloni, J. Pastorek, S. Pastorekova, C. Pedone, A. Scozzafava, S. M. Monti, and G. De Simone. 2009. 'Crystal structure of the catalytic domain of the tumor-associated human carbonic anhydrase IX', *Proc Natl Acad Sci U S A*, 106: 16233-8.
- Ames, S., S. Pastorekova, and H. M. Becker. 2018. 'The proteoglycan-like domain of carbonic anhydrase IX mediates non-catalytic facilitation of lactate transport in cancer cells', *Oncotarget*, 9: 27940-57.
- Anduran, E., A. Aspatwar, N. K. Parvathaneni, D. Suylen, S. Bua, A. Nocentini, S. Parkkila, C. T. Supuran, L. Dubois, P. Lambin, and J. Y. Winum. 2020. 'Hypoxia-Activated Prodrug Derivatives of Carbonic Anhydrase Inhibitors in Benzenesulfonamide Series: Synthesis and Biological Evaluation', *Molecules*, 25.
- Barathova, M., M. Takacova, T. Holotnakova, A. Gibadulinova, A. Ohradanova, M. Zatovicova, A. Hulikova, J. Kopacek, S. Parkkila, C. T. Supuran, S. Pastorekova, and J. Pastorek. 2008. 'Alternative splicing variant of the hypoxia marker carbonic anhydrase IX expressed independently of hypoxia and tumour phenotype', *Br J Cancer*, 98: 129-36.
- Bednenko, J., G. Cingolani, and L. Gerace. 2003. 'Nucleocytoplasmic transport: navigating the channel', *Traffic*, 4: 127-35.
- Bleumer, I., A. Knuth, E. Oosterwijk, R. Hofmann, Z. Varga, C. Lamers, W. Kruit, S. Melchior, C. Mala, S. Ullrich, P. De Mulder, P. F. Mulders, and J. Beck. 2004. 'A phase II trial of chimeric monoclonal antibody

- G250 for advanced renal cell carcinoma patients', *Br J Cancer*, 90: 985-90.
- Brand, T. M., M. Iida, N. Luthar, M. M. Starr, E. J. Huppert, and D. L. Wheeler. 2013. 'Nuclear EGFR as a molecular target in cancer', *Radiother Oncol*, 108: 370-7.
- Bryant, K. L., B. Baird, and D. Holowka. 2015. 'A novel fluorescence-based biosynthetic trafficking method provides pharmacologic evidence that PI4-kinase IIIalpha is important for protein trafficking from the endoplasmic reticulum to the plasma membrane', *BMC Cell Biol*, 16: 5.
- Bua, S., L. Di Cesare Mannelli, D. Vullo, C. Ghelardini, G. Bartolucci, A. Scozzafava, C. T. Supuran, and F. Carta. 2017. 'Design and Synthesis of Novel Nonsteroidal Anti-Inflammatory Drugs and Carbonic Anhydrase Inhibitors Hybrids (NSAIDs-CAIs) for the Treatment of Rheumatoid Arthritis', *J Med Chem*, 60: 1159-70.
- Buane, P., G. Renzone, F. Monteleone, M. Vitale, S. M. Monti, A. Sandomenico, C. Garbi, D. Montanaro, M. Accardo, G. Troncone, M. Zatovicova, L. Csaderova, C. T. Supuran, S. Pastorekova, A. Scaloni, G. De Simone, and N. Zambrano. 2013. 'Characterization of carbonic anhydrase IX interactome reveals proteins assisting its nuclear localization in hypoxic cells', *J Proteome Res*, 12: 282-92.
- Bulli, I., I. Dettori, E. Coppi, F. Cherchi, M. Venturini, L. Di Cesare Mannelli, C. Ghelardini, A. Nocentini, C. T. Supuran, A. M. Pugliese, and F. Pedata. 2021. 'Role of Carbonic Anhydrase in Cerebral Ischemia and Carbonic Anhydrase Inhibitors as Putative Protective Agents', *Int J Mol Sci*, 22.
- Buonanno, M., E. Langella, N. Zambrano, M. Succoio, E. Sasso, V. Alterio, A. Di Fiore, A. Sandomenico, C. T. Supuran, A. Scaloni, S. M. Monti, and G. De Simone. 2017. 'Disclosing the Interaction of Carbonic Anhydrase IX with Cullin-Associated NEDD8-Dissociated Protein 1

- by Molecular Modeling and Integrated Binding Measurements', *ACS Chem Biol*, 12: 1460-65.
- Conner, D. A. 2001. 'Mouse embryo fibroblast (MEF) feeder cell preparation', *Curr Protoc Mol Biol*, Chapter 23: Unit 23 2.
- Conti, E., C. W. Muller, and M. Stewart. 2006. 'Karyopherin flexibility in nucleocytoplasmic transport', *Curr Opin Struct Biol*, 16: 237-44.
- De Craene, J. O., D. L. Bertazzi, S. Bar, and S. Friant. 2017. 'Phosphoinositides, Major Actors in Membrane Trafficking and Lipid Signaling Pathways', *Int J Mol Sci*, 18.
- De Simone, G., V. Alterio, and C. T. Supuran. 2013. 'Exploiting the hydrophobic and hydrophilic binding sites for designing carbonic anhydrase inhibitors', *Expert Opin Drug Discov*, 8: 793-810.
- Di Cesare Mannelli, L., L. Micheli, F. Carta, A. Cozzi, C. Ghelardini, and C. T. Supuran. 2016. 'Carbonic anhydrase inhibition for the management of cerebral ischemia: in vivo evaluation of sulfonamide and coumarin inhibitors', *J Enzyme Inhib Med Chem*, 31: 894-9.
- Doherty, G. J., and H. T. McMahon. 2009. 'Mechanisms of endocytosis', *Annu Rev Biochem*, 78: 857-902.
- Donaldson, J. G., and C. L. Jackson. 2011. 'ARF family G proteins and their regulators: roles in membrane transport, development and disease', *Nat Rev Mol Cell Biol*, 12: 362-75.
- Duda, D. M., D. C. Scott, M. F. Calabrese, E. S. Zimmerman, N. Zheng, and B. A. Schulman. 2011. 'Structural regulation of cullin-RING ubiquitin ligase complexes', *Curr Opin Struct Biol*, 21: 257-64.
- Erra Diaz, F., E. Dantas, and J. Geffner. 2018. 'Unravelling the Interplay between Extracellular Acidosis and Immune Cells', *Mediators Inflamm*, 2018: 1218297.
- Faini, M., R. Beck, F. T. Wieland, and J. A. Briggs. 2013. 'Vesicle coats: structure, function, and general principles of assembly', *Trends Cell Biol*, 23: 279-88.

- Gadde, K. M., D. M. Francis, H. R. Wagner, 2nd, and K. R. Krishnan. 2003. 'Zonisamide for weight loss in obese adults: a randomized controlled trial', *JAMA*, 289: 1820-5.
- Gillies, R. J., and R. A. Gatenby. 2015. 'Metabolism and its sequelae in cancer evolution and therapy', *Cancer J*, 21: 88-96.
- Gomez-Navarro, N., and E. Miller. 2016. 'Protein sorting at the ER-Golgi interface', *J Cell Biol*, 215: 769-78.
- Grossman, E., O. Medalia, and M. Zwerger. 2012. 'Functional architecture of the nuclear pore complex', *Annu Rev Biophys*, 41: 557-84.
- Gut, M. O., S. Parkkila, Z. Vernerova, E. Rohde, J. Zavada, M. Hocker, J. Pastorek, T. Karttunen, A. Gibadulinova, Z. Zavadova, K. P. Knobeloch, B. Wiedenmann, J. Svoboda, I. Horak, and S. Pastorekova. 2002. 'Gastric hyperplasia in mice with targeted disruption of the carbonic anhydrase gene Car9', *Gastroenterology*, 123: 1889-903.
- Harris, A. L. 2002. 'Hypoxia--a key regulatory factor in tumour growth', *Nat Rev Cancer*, 2: 38-47.
- Hilvo, M., L. Baranauskienė, A. M. Salzano, A. Scaloni, D. Matulis, A. Innocenti, A. Scozzafava, S. M. Monti, A. Di Fiore, G. De Simone, M. Lindfors, J. Janis, J. Valjakka, S. Pastorekova, J. Pastorek, M. S. Kulomaa, H. R. Nordlund, C. T. Supuran, and S. Parkkila. 2008. 'Biochemical characterization of CA IX, one of the most active carbonic anhydrase isozymes', *J Biol Chem*, 283: 27799-809.
- Hoelz, A., E. W. Debler, and G. Blobel. 2011. 'The structure of the nuclear pore complex', *Annu Rev Biochem*, 80: 613-43.
- Huang, L. E., and H. F. Bunn. 2003. 'Hypoxia-inducible factor and its biomedical relevance', *J Biol Chem*, 278: 19575-8.
- Hulikova, A., M. Zatovcova, E. Svastova, P. Ditte, R. Brasseur, R. Kettmann, C. T. Supuran, J. Kopacek, J. Pastorek, and S. Pastorekova. 2009. 'Intact intracellular tail is critical for proper functioning of the tumor-

- associated, hypoxia-regulated carbonic anhydrase IX', *FEBS Lett*, 583: 3563-8.
- Ikonen, E., and K. Simons. 1998. 'Protein and lipid sorting from the trans-Golgi network to the plasma membrane in polarized cells', *Semin Cell Dev Biol*, 9: 503-9.
- Ilardi, G., N. Zambrano, F. Merolla, M. Siano, S. Varricchio, M. Vecchione, G. De Rosa, M. Mascolo, and S. Staibano. 2014. 'Histopathological determinants of tumor resistance: a special look to the immunohistochemical expression of carbonic anhydrase IX in human cancers', *Curr Med Chem*, 21: 1569-82.
- Jamali, S., M. Klier, S. Ames, L. F. Barros, R. McKenna, J. W. Deitmer, and H. M. Becker. 2015. 'Hypoxia-induced carbonic anhydrase IX facilitates lactate flux in human breast cancer cells by non-catalytic function', *Sci Rep*, 5: 13605.
- Jena, B. P. 2011. 'Role of SNAREs in membrane fusion', *Adv Exp Med Biol*, 713: 13-32.
- Kaluz, S., M. Kaluzova, S. Y. Liao, M. Lerman, and E. J. Stanbridge. 2009. 'Transcriptional control of the tumor- and hypoxia-marker carbonic anhydrase 9: A one transcription factor (HIF-1) show?', *Biochim Biophys Acta*, 1795: 162-72.
- Kaluz, S., M. Kaluzova, R. Opavsky, S. Pastorekova, A. Gibadulinova, F. Dequiedt, R. Kettmann, and J. Pastorek. 1999. 'Transcriptional regulation of the MN/CA 9 gene coding for the tumor-associated carbonic anhydrase IX. Identification and characterization of a proximal silencer element', *J Biol Chem*, 274: 32588-95.
- Kciuk, M., A. Gielecinska, S. Mujwar, M. Mojzych, B. Marciniak, R. Drozda, and R. Kontek. 2022. 'Targeting carbonic anhydrase IX and XII isoforms with small molecule inhibitors and monoclonal antibodies', *J Enzyme Inhib Med Chem*, 37: 1278-98.

- Krasavin, M., S. Kalinin, T. Sharonova, and C. T. Supuran. 2020. 'Inhibitory activity against carbonic anhydrase IX and XII as a candidate selection criterion in the development of new anticancer agents', *J Enzyme Inhib Med Chem*, 35: 1555-61.
- Kutay, U., and S. Guttinger. 2005. 'Leucine-rich nuclear-export signals: born to be weak', *Trends Cell Biol*, 15: 121-4.
- Lardner, A. 2001. 'The effects of extracellular pH on immune function', *J Leukoc Biol*, 69: 522-30.
- Lee, M. C., E. A. Miller, J. Goldberg, L. Orci, and R. Schekman. 2004. 'Bi-directional protein transport between the ER and Golgi', *Annu Rev Cell Dev Biol*, 20: 87-123.
- Leisegang, M. S., R. Martin, A. S. Ramirez, and M. T. Bohnsack. 2012. 'Exportin t and Exportin 5: tRNA and miRNA biogenesis - and beyond', *Biol Chem*, 393: 599-604.
- Lippincott-Schwartz, J., L. C. Yuan, J. S. Bonifacino, and R. D. Klausner. 1989. 'Rapid redistribution of Golgi proteins into the ER in cells treated with brefeldin A: evidence for membrane cycling from Golgi to ER', *Cell*, 56: 801-13.
- Liu, F., and L. D. McCullough. 2014. 'The middle cerebral artery occlusion model of transient focal cerebral ischemia', *Methods Mol Biol*, 1135: 81-93.
- Margheri, F., M. Ceruso, F. Carta, A. Laurenzana, L. Maggi, S. Lazzeri, G. Simonini, F. Annunziato, M. Del Rosso, C. T. Supuran, and R. Cimaz. 2016. 'Overexpression of the transmembrane carbonic anhydrase isoforms IX and XII in the inflamed synovium', *J Enzyme Inhib Med Chem*, 31: 60-63.
- McDonald, P. C., S. Chia, P. L. Bedard, Q. Chu, M. Lyle, L. Tang, M. Singh, Z. Zhang, C. T. Supuran, D. J. Renouf, and S. Dedhar. 2020. 'A Phase 1 Study of SLC-0111, a Novel Inhibitor of Carbonic Anhydrase IX,

- in Patients With Advanced Solid Tumors', *Am J Clin Oncol*, 43: 484-90.
- McDonald, P. C., M. Swayampakula, and S. Dedhar. 2018. 'Coordinated Regulation of Metabolic Transporters and Migration/Invasion by Carbonic Anhydrase IX', *Metabolites*, 8.
- McLane, L. M., and A. H. Corbett. 2009. 'Nuclear localization signals and human disease', *IUBMB Life*, 61: 697-706.
- Mellman, I., and G. Warren. 2000. 'The road taken: past and future foundations of membrane traffic', *Cell*, 100: 99-112.
- Misumi, Y., Y. Misumi, K. Miki, A. Takatsuki, G. Tamura, and Y. Ikehara. 1986. 'Novel blockade by brefeldin A of intracellular transport of secretory proteins in cultured rat hepatocytes', *J Biol Chem*, 261: 11398-403.
- Morgan, P. E., S. Pastorekova, A. K. Stuart-Tilley, S. L. Alper, and J. R. Casey. 2007. 'Interactions of transmembrane carbonic anhydrase, CAIX, with bicarbonate transporters', *Am J Physiol Cell Physiol*, 293: C738-48.
- Mussi, S., S. Rezzola, P. Chiodelli, A. Nocentini, C. T. Supuran, and R. Ronca. 2022. 'Antiproliferative effects of sulphonamide carbonic anhydrase inhibitors C18, SLC-0111 and acetazolamide on bladder, glioblastoma and pancreatic cancer cell lines', *J Enzyme Inhib Med Chem*, 37: 280-86.
- Nakagawa, Y., H. Uemura, Y. Hirao, K. Yoshida, S. Saga, and K. Yoshikawa. 1998. 'Radiation hybrid mapping of the human MN/CA9 locus to chromosome band 9p12-p13', *Genomics*, 53: 118-9.
- Neri, D., and C. T. Supuran. 2011. 'Interfering with pH regulation in tumours as a therapeutic strategy', *Nat Rev Drug Discov*, 10: 767-77.
- Opavsky, R., S. Pastorekova, V. Zelnik, A. Gibadulinova, E. J. Stanbridge, J. Zavada, R. Kettmann, and J. Pastorek. 1996. 'Human MN/CA9 gene,

- a novel member of the carbonic anhydrase family: structure and exon to protein domain relationships', *Genomics*, 33: 480-7.
- Parks, S. K., J. Chiche, and J. Pouyssegur. 2011. 'pH control mechanisms of tumor survival and growth', *J Cell Physiol*, 226: 299-308.
- Pastorekova, S., and R. J. Gillies. 2019. 'The role of carbonic anhydrase IX in cancer development: links to hypoxia, acidosis, and beyond', *Cancer Metastasis Rev*, 38: 65-77.
- Pastorekova, S., M. Zatovicova, and J. Pastorek. 2008. 'Cancer-associated carbonic anhydrases and their inhibition', *Curr Pharm Des*, 14: 685-98.
- Pfeffer, S. R. 2013. 'Rab GTPase regulation of membrane identity', *Curr Opin Cell Biol*, 25: 414-9.
- . 2017. 'Rab GTPases: master regulators that establish the secretory and endocytic pathways', *Mol Biol Cell*, 28: 712-15.
- Picard, F., Y. Deshaies, J. Lalonde, P. Samson, and D. Richard. 2000. 'Topiramate reduces energy and fat gains in lean (Fa/?) and obese (fa/fa) Zucker rats', *Obes Res*, 8: 656-63.
- Pignataro, G., E. Esposito, O. Cuomo, R. Sirabella, F. Boscia, N. Guida, G. Di Renzo, and L. Annunziato. 2011. 'The NCX3 isoform of the Na⁺/Ca²⁺ exchanger contributes to neuroprotection elicited by ischemic postconditioning', *J Cereb Blood Flow Metab*, 31: 362-70.
- Pignataro, G., F. E. Studer, A. Wilz, R. P. Simon, and D. Boison. 2007. 'Neuroprotection in ischemic mouse brain induced by stem cell-derived brain implants', *J Cereb Blood Flow Metab*, 27: 919-27.
- Plum, F. 1983. 'What causes infarction in ischemic brain?: The Robert Wartenberg Lecture', *Neurology*, 33: 222-33.
- Raghunand, N., R. A. Gatenby, and R. J. Gillies. 2003. 'Microenvironmental and cellular consequences of altered blood flow in tumours', *Br J Radiol*, 76 Spec No 1: S11-22.

- Rahmani, K., and D. A. Dean. 2017. 'Leptomycin B alters the subcellular distribution of CRM1 (Exportin 1)', *Biochem Biophys Res Commun*, 488: 253-58.
- Riihonen, R., C. T. Supuran, S. Parkkila, S. Pastorekova, H. K. Vaananen, and T. Laitala-Leinonen. 2007. 'Membrane-bound carbonic anhydrases in osteoclasts', *Bone*, 40: 1021-31.
- Rohani, N., L. Hao, M. S. Alexis, B. A. Joughin, K. Krismer, M. N. Moufarrej, A. R. Soltis, D. A. Lauffenburger, M. B. Yaffe, C. B. Burge, S. N. Bhatia, and F. B. Gertler. 2019. 'Acidification of Tumor at Stromal Boundaries Drives Transcriptome Alterations Associated with Aggressive Phenotypes', *Cancer Res*, 79: 1952-66.
- Sasso, E., M. Vitale, F. Monteleone, F. L. Boffo, M. Santoriello, D. Sarnataro, C. Garbi, M. Sabatella, B. Crifo, L. A. Paoletta, G. Minopoli, J. Y. Winum, and N. Zambrano. 2015. 'Binding of carbonic anhydrase IX to 45S rDNA genes is prevented by exportin-1 in hypoxic cells', *Biomed Res Int*, 2015: 674920.
- Siebels, M., K. Rohrman, R. Oberneder, M. Stahler, N. Haseke, J. Beck, R. Hofmann, M. Kindler, P. Kloepfer, and C. Stief. 2011. 'A clinical phase I/II trial with the monoclonal antibody cG250 (RENCAREX(R)) and interferon-alpha-2a in metastatic renal cell carcinoma patients', *World J Urol*, 29: 121-6.
- Sisalli, M. J., A. Secondo, A. Esposito, V. Valsecchi, C. Savoia, G. F. Di Renzo, L. Annunziato, and A. Scorziello. 2014. 'Endoplasmic reticulum refilling and mitochondrial calcium extrusion promoted in neurons by NCX1 and NCX3 in ischemic preconditioning are determinant for neuroprotection', *Cell Death Differ*, 21: 1142-9.
- Stanley, P. 2011. 'Golgi glycosylation', *Cold Spring Harb Perspect Biol*, 3.
- Stenmark, H. 2009. 'Rab GTPases as coordinators of vesicle traffic', *Nat Rev Mol Cell Biol*, 10: 513-25.

- Sugrue, M. F. 2000. 'Pharmacological and ocular hypotensive properties of topical carbonic anhydrase inhibitors', *Prog Retin Eye Res*, 19: 87-112.
- Supuran, C. T. 2008. 'Carbonic anhydrases: novel therapeutic applications for inhibitors and activators', *Nat Rev Drug Discov*, 7: 168-81.
- . 2016a. 'How many carbonic anhydrase inhibition mechanisms exist?', *J Enzyme Inhib Med Chem*, 31: 345-60.
- . 2016b. 'Structure and function of carbonic anhydrases', *Biochem J*, 473: 2023-32.
- . 2021. 'Carbonic anhydrase inhibitors: an update on experimental agents for the treatment and imaging of hypoxic tumors', *Expert Opin Investig Drugs*, 30: 1197-208.
- Supuran, C. T., V. Alterio, A. Di Fiore, D' Ambrosio K, F. Carta, S. M. Monti, and G. De Simone. 2018. 'Inhibition of carbonic anhydrase IX targets primary tumors, metastases, and cancer stem cells: Three for the price of one', *Med Res Rev*, 38: 1799-836.
- Supuran, C. T., A. Di Fiore, V. Alterio, S. M. Monti, and G. De Simone. 2010. 'Recent advances in structural studies of the carbonic anhydrase family: the crystal structure of human CA IX and CA XIII', *Curr Pharm Des*, 16: 3246-54.
- Svastova, E., A. Hulikova, M. Rafajova, M. Zat'ovicova, A. Gibadulinova, A. Casini, A. Cecchi, A. Scozzafava, C. T. Supuran, J. Pastorek, and S. Pastorekova. 2004. 'Hypoxia activates the capacity of tumor-associated carbonic anhydrase IX to acidify extracellular pH', *FEBS Lett*, 577: 439-45.
- Svastova, E., W. Witariski, L. Csaderova, I. Kosik, L. Skvarkova, A. Hulikova, M. Zatovicova, M. Barathova, J. Kopacek, J. Pastorek, and S. Pastorekova. 2012. 'Carbonic anhydrase IX interacts with bicarbonate transporters in lamellipodia and increases cell migration via its catalytic domain', *J Biol Chem*, 287: 3392-402.

- Svastova, E., N. Zilka, M. Zat'ovicova, A. Gibadulinova, F. Ciampor, J. Pastorek, and S. Pastorekova. 2003. 'Carbonic anhydrase IX reduces E-cadherin-mediated adhesion of MDCK cells via interaction with beta-catenin', *Exp Cell Res*, 290: 332-45.
- Swietach, P., A. Hulikova, R. D. Vaughan-Jones, and A. L. Harris. 2010. 'New insights into the physiological role of carbonic anhydrase IX in tumour pH regulation', *Oncogene*, 29: 6509-21.
- Trullas, J. C., J. L. Morales-Rull, and F. Formiga. 2014. '[Diuretic therapy in acute heart failure]', *Med Clin (Barc)*, 142 Suppl 1: 36-41.
- Tuettenberg, J., A. Heimann, and O. Kempfski. 2001. 'Nitric oxide modulates cerebral blood flow stimulation by acetazolamide in the rat cortex: a laser Doppler scanning study', *Neurosci Lett*, 315: 65-8.
- Vander Heiden, M. G., L. C. Cantley, and C. B. Thompson. 2009. 'Understanding the Warburg effect: the metabolic requirements of cell proliferation', *Science*, 324: 1029-33.
- Wang, Y. N., and M. C. Hung. 2012. 'Nuclear functions and subcellular trafficking mechanisms of the epidermal growth factor receptor family', *Cell Biosci*, 2: 13.
- Weis, K. 2002. 'Nucleocytoplasmic transport: cargo trafficking across the border', *Curr Opin Cell Biol*, 14: 328-35.
- . 2003. 'Regulating access to the genome: nucleocytoplasmic transport throughout the cell cycle', *Cell*, 112: 441-51.
- Williamson, M. R., C. M. Wilkinson, K. Dietrich, and F. Colbourne. 2019. 'Acetazolamide Mitigates Intracranial Pressure Spikes Without Affecting Functional Outcome After Experimental Hemorrhagic Stroke', *Transl Stroke Res*, 10: 428-39.
- Wykoff, C. C., N. J. Beasley, P. H. Watson, K. J. Turner, J. Pastorek, A. Sibtain, G. D. Wilson, H. Turley, K. L. Talks, P. H. Maxwell, C. W. Pugh, P. J. Ratcliffe, and A. L. Harris. 2000. 'Hypoxia-inducible

expression of tumor-associated carbonic anhydrases', *Cancer Res*, 60: 7075-83.

Zatovicova, M., L. Jelenska, A. Hulikova, L. Csaderova, Z. Ditte, P. Ditte, T. Goliasova, J. Pastorek, and S. Pastorekova. 2010. 'Carbonic anhydrase IX as an anticancer therapy target: preclinical evaluation of internalizing monoclonal antibody directed to catalytic domain', *Curr Pharm Des*, 16: 3255-63.

Book with authors

Alberts, Bruce. 2015. *Molecular biology of the cell* (Garland Science, Taylor and Francis Group: New York, NY).

8. Publications

Gentile, C.; Finizio, A.; Froehlich, G.; D'Alise, A.M.; Cotugno, G.; Amiranda, S.; Nicosia, A.; Scarselli, E.; Zambrano, N.; Sasso, E. Generation of a Retargeted Oncolytic *Herpes* Virus Encoding Adenosine Deaminase for Tumor Adenosine Clearance. *Int. J. Mol. Sci.* **2021**, *22*, 13521. <https://doi.org/10.3390/ijms222413521>

Miro, C.; Nappi, A.; Cicatiello, A.G.; Di Cicco, E.; Saggiocchi, S.; Murolo, M.; Belli, V.; Troiani, T.; Albanese, S.; Amiranda, S.; Zavacki, A.M.; Stornaiuolo, M.; Mancini, M.; Salvatore, D.; Dentice, M. Thyroid Hormone Enhances Angiogenesis and the Warburg Effect in Squamous Cell Carcinomas. *Cancers* **2021**, *13*, 2743. <https://doi.org/10.3390/cancers13112743>

Succoio, M. and Amiranda, S. (co-first); Marciano, C.; Sasso, E.; De Simone, G.; Garbi, C.; Zambrano, N. The C-terminal protein interaction domain of Carbonic anhydrase IX is required for proper localization of the protein in mammalian cells. Manuscript in preparation.

Succoio, M. and Amiranda, S.; Zambrano N (Department of Molecular Medicine and Medical Biotechnology, University of Naples Federico II); Pignataro, G.; Secondo, A.; et al. (Department of Neuroscience and Reproductive and Odontostomatological Sciences, University of Naples Federico II). Carbonic anhydrase IX contributes to hypoxia/reperfusion damage in rodent models of cerebral ischemia. Full Author list under definition, Manuscript in preparation.

Froehlich, G.; Napolano, A.; Finizio A.; Amiranda, S.; De Chiara, A.; Zambrano, N.; Sasso, E. Single nucleotide polymorphisms in Tmem173 gene affect functionality of STING in monocytes maturation and non-immune cells response to viruses. Full Author list under definition, Manuscript in preparation.

Poster presentation at National Ph.D. Meeting (24-26 March 2022, Salerno, Italy) Amiranda S., Succoio M., Marciano C., Finizio A., De Simone G., Sasso E., Garbi C., Zambrano N. Mutations in the protein interaction motifs of carbonic anhydrase IX alter its intracellular trafficking in hypoxic cells.